Regulation of DEPTOR Ubiquitination by Uric Acid in the Pancreatic β-Cell

By Ethan C. J. Cain

Supervisor: Dr. Andrew Bahn

Abstract

As rates of non-communicable disease such as diabetes mellitus raise the questions regarding how these diseases arise becomes more pertinent. One of the major causes of these types of disease is the effects of the modern diet which is typically high in nutrients including sugars, fats, purines and salt. Of these nutrients, the effects of high purines have been underrepresented in the current body of research. Increased dietary purines result in a commensurate increase in the synthesis of uric acid elevating serum uric acid level. This increase induces hyperuricemia and has been correlated through epidemiological studies to the development and progression of degenerative diseases including diabetes mellitus.

In an attempt to shed light on the mechanism that underpins this effect we have elected to investigate the effects of hyperuricemic conditions on the viability and growth of pancreatic β-cells through the use of live cell assays to evaluate: cellular metabolism, cell count, autophagy, and apoptosis. To explain any changes in pancreatic β-cell viability and proliferation, we also investigated how the stability of a cellular growth and viability regulating protein, DEPTOR, may change under hyperuricemic conditions. We did this by directly measuring DEPTOR-bound ubiquitin though the use of co-immunoprecipitation. To explain any observed changes in DEPTOR ubiquitination we also investigated the expression of proteins responsible for DEPTOR ubiquitination, β-TrCP, and DEPTOR deubiquitination, USP3. Finally, we investigated if there was any direct interaction between DEPTOR and uric acid using co-immunoprecipitation to test for any potential bound uric acid as it may provide insights into any changes in DEPTOR ubiquitination, β-TrCP expression, or USP3 expression.

As a result of this investigation, we found that hyperuricemic conditions are sufficient to cause significant reductions in pancreatic β-cell metabolism and cell mass and a significant increase in

autophagy and apoptosis. This was paired with an increase in DEPTOR stability arising from the observed reduction in DEPTOR-bound ubiquitin. This reduction in DEPTOR-bound ubiquitin was caused by a significant shift in the expression of β-TrCP and USP3 which resulted in a net shift in the balance if ubiquitination to favour the removal of ubiquitin over its binding. Additionally, our attempts to probe for potential DEPTOR-bound uric acid were successful and found that uric acid did in fact bind to DEPTOR and that this binding may explain what initiated the shifted balance of DEPTOR ubiquitination.

These results have presented some interesting questions as they are the first to indicate: uric acid is capable of modifying DEPTOR ubiquitination, USP3 was identified as a new major regulator of DEPTOR stability within the pancreatic β-cell, uric acid as a possible new regulator of cell function that has as yet gone unnoticed, and finally the differences between mouse and human responses to hyperuricemia may provide new insights into the potential mechanism that underpins uric acid's role in the regulation of ubiquitination.

In summary, in our attempts to better understand the causes of uric acid driven increases in diabetes mellitus risk we have found that hyperuricemic conditions are sufficient to reduce the function and mass of pancreatic β-cells and that this effect is caused by a previously undescribed uric acid-driven change in regulatory protein levels.

Acknowledgements

To begin my acknowledgements, I would like to thank my supervisor Dr Andrew Bahn without whom none of my research would have been possible. I would like to thank him for providing me with the opportunity to develop my skills as a researcher and pursue scientific research. I would also like to thank him for going above and beyond to provide support to allow me to achieve all that you will see within this thesis even in the face of my excessive procrastination.

In addition to Andrew, I would also like to thank my advisor Dr Regis Lamberts for his help throughout my time as a master's student. Also, the fellow members of the Bahn laboratory for providing some much-needed distractions and assistance throughout the course of my thesis.

I would like to thank my friends and family; without their support, I would surely have lost what remains of my tenuous grip on sanity and for their encouragement through some of the more frustrating periods of my experiment.

Finally, I would like to thank the students and the staff of the department for all their assistance and understanding throughout the course of the year.

Table of contents

Contents

List of Figures

List of Tables

Abbreviations

4E-BP1	**4E-binding protein 1**
ABCG2	**ATP-binding cassette sub-family G member 2**
ADP	**adenosine diphosphate**
Akt	**serine-threonine kinase**
AMP	**adenosine monophosphate**
AMPK	**AMP-dependent kinase**
ATP	**adenosine triphosphate**
β-TrCP	**Beta-transducin repeat containing**
Ca^{2+}	**calcium ion**
cDNA	**complementary DNA**
CO_2	**carbon dioxide**
DEPTOR	**DEP domain containing mTOR interacting protein**
DUB	**Deubiquitinating enzyme**
dH_2O	**distilled water**
DNA	**deoxyribonucleic acid**
DM	**diabetes mellitus**
DMSO	**dimethyl-sulfoxide**
FBS	**fetal bovine serum**
FKBP-12	**peptidyl-prolyl cis-trans isomerase FKBP1A**
GLUT1	**glucose transporter 1**
GLUT2	**glucose transporter 2**
GLUT9	**glucose transporter 9**
H_2O	**water**
HCl	**hydrochloric acid**
mLST8	**Target of rapamycin complex subunit LST8**
MRP4	**multi-drug resistant protein 4**

mRNA	**messenger-RNA**
mTOR	**mechanistic target of rapamycin**
MTT	**3-(4,5-dimethylthiazol-2-yl)-2,5-diphenyltetrazolium bromide**
$NaHCO_3$	**sodium bicarbonate**
OAT1-4	**organic anion transporter 1-4**
PBS	**phosphate-buffered saline**
PCR	**polymerase chain reaction**
RNA	**ribonucleic acid**
RIPA	**radioimmunoprecipitation buffer**
rRNA	**ribosomal RNA**
ROS	**reactive oxygen species**
RPM	**revolutions per minute**
S6K1	**S6 Kinase 1**
SEM	**standard error of the mean**
SGK	**serine/threonine-protein kinases**
SUA	**serum uric acid**
T1DM	**type-1 diabetes mellitus**
T2DM	**type-2 diabetes mellitus**
TBST	**tris-buffered saline-tween 20**
TSC2	**tuberous sclerosis complex 2**
USP	**Ubiquitin Specific Protease**
USP3	**Ubiquitin Specific Protease 3**
URAT1	**uric acid transporter 1**
XO	**xanthine oxidase**

Introduction

1.1 Uric acid

1.1.1 Uric acid homeostasis

In humans, uric acid is the final product of purine metabolism. It takes place in all cells as the regulation of purines is key to maintaining adequate regulation of DNA, RNA and ATP functions, however, uric acid is mainly synthesised in the liver from purines and the metabolism of dietary fructose (Fathallah-Shaykh & Cramer, 2014). As shown in figure 1 uric acid synthesis is performed by the enzyme xanthine oxidase (XO) which acts as a rate limiting enzyme (Maiuolo et al., 2016). Uric acid leaves the body by excretion via the kidney or the intestine. The kidney is an important regulator of circulating uric acid levels as it reabsorbs around 90% of filtered uric acid whilst being responsible for 60–70% of total body uric acid excretion (Bobulescu & Moe, 2012). This is achieved via uric acid transporters namely ATP-binding cassette superfamily G member 2 (ABCG2), solute carrier family 2 member 9 (GLUT9), multidrug resistance-associated protein 4 (MRP4), organic anion transporters 1-4 (OAT1-4), and solute carrier family 22 member 12 (URAT1), all of which as shown in figure 2 are found within the proximal tubule, and act to maintain dynamic uric acid homeostasis (Wright et al., 2010).

1.1.2 What is hyperuricemia and how does it arise?

Hyperuricemia is a condition, defined clinically as a serum uric acid (SUA) level exceeding 6.5 mg/dL (360μM) and can occur in many ways. The primary form as the more common form is due to increased purine metabolism and is resulting from dietary and lifestyle factors (So & Thorens, 2010). Secondary hyperuricemia is caused by dysregulation of normal uric acid homeostasis due to diseases like chronic renal disease (Kelly *et al.*, 1973), including increased xanthine oxidase function or changes in the function of excretory pathways. Primary hyperuricemia has seen a massive rise in recent years as modern diets with increased purine levels, sugars (particularly

fructose) and more sedentary lifestyles lead to growing incidence rates of hyperuricemia worldwide (Zhu et al., 2011).

Considering this trend, there has been increased interest in studying the effects of hyperuricemia beyond uric acid crystallisation leading to gout. These studies focus primarily on how serum uric acid may modify existing cellular survival pathways such as how uric acid can increase autophagy through upregulation of Microtubule-associated proteins 1A/1B light chain 3B (LC3-II) (Sheng *et al.*, 2017) and how it increases inflammatory response through the upregulation of nuclear factor-κB (NF-κB) (Spiga *et al.*, 2017). This research has prompted investigation into how the resultant changes induced by hyperuricemia may impact on diseases that arise from a diet similar to that of a high purine diet such as a high fat or high sugar diet, namely diabetes mellitus.

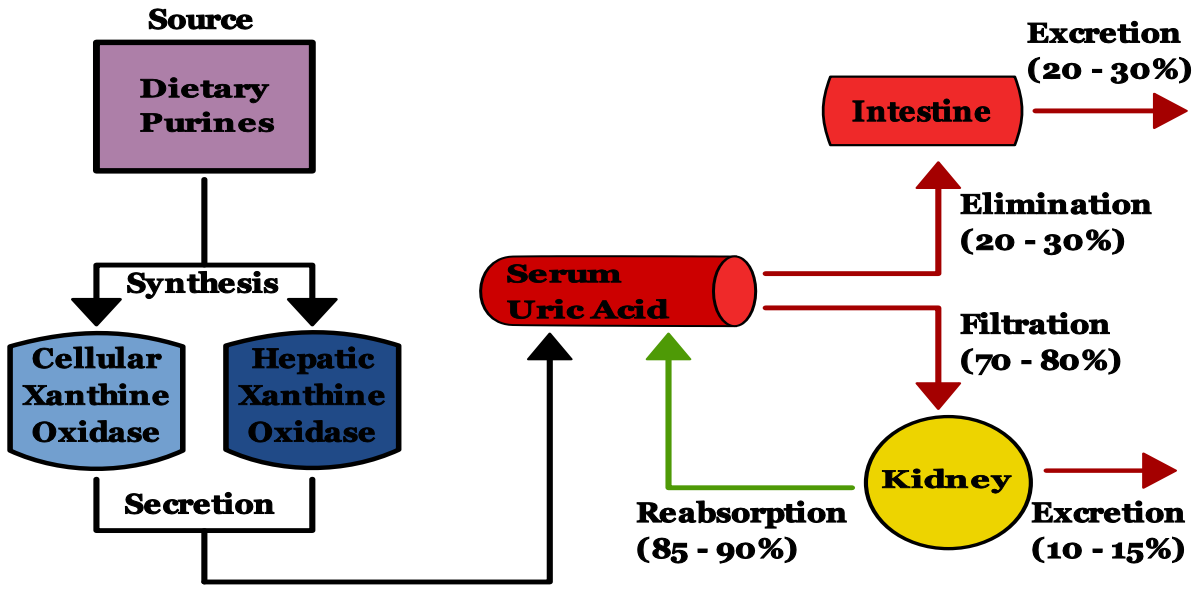

Figure 1. A schematic representation of normal human uric acid homeostasis.
In humans, uric acid is produced by the breakdown of purines which are obtained primarily through dietary intake. Purines metabolites are then converted to uric acid by the enzyme xanthine oxidase within the cell. The highest concentrations of xanthine oxidase is found in the liver. Following its synthesis uric acid is secreted into to the bloodstream where it accumulates and can be measured as serum uric acid. Uric acid levels within the serum are a result of the balance between its synthesis and excretion. The majority of the uric acid excretion is handled by the kidney which filters 70 - 80 % of the serum uric acid, of which 10 - 15% is excreted and the remaining 85 – 90% is reabsorbed. The 20 – 30 % of serum uric acid that is not eliminated by the kidneys is eliminated via excretion by the intestine.

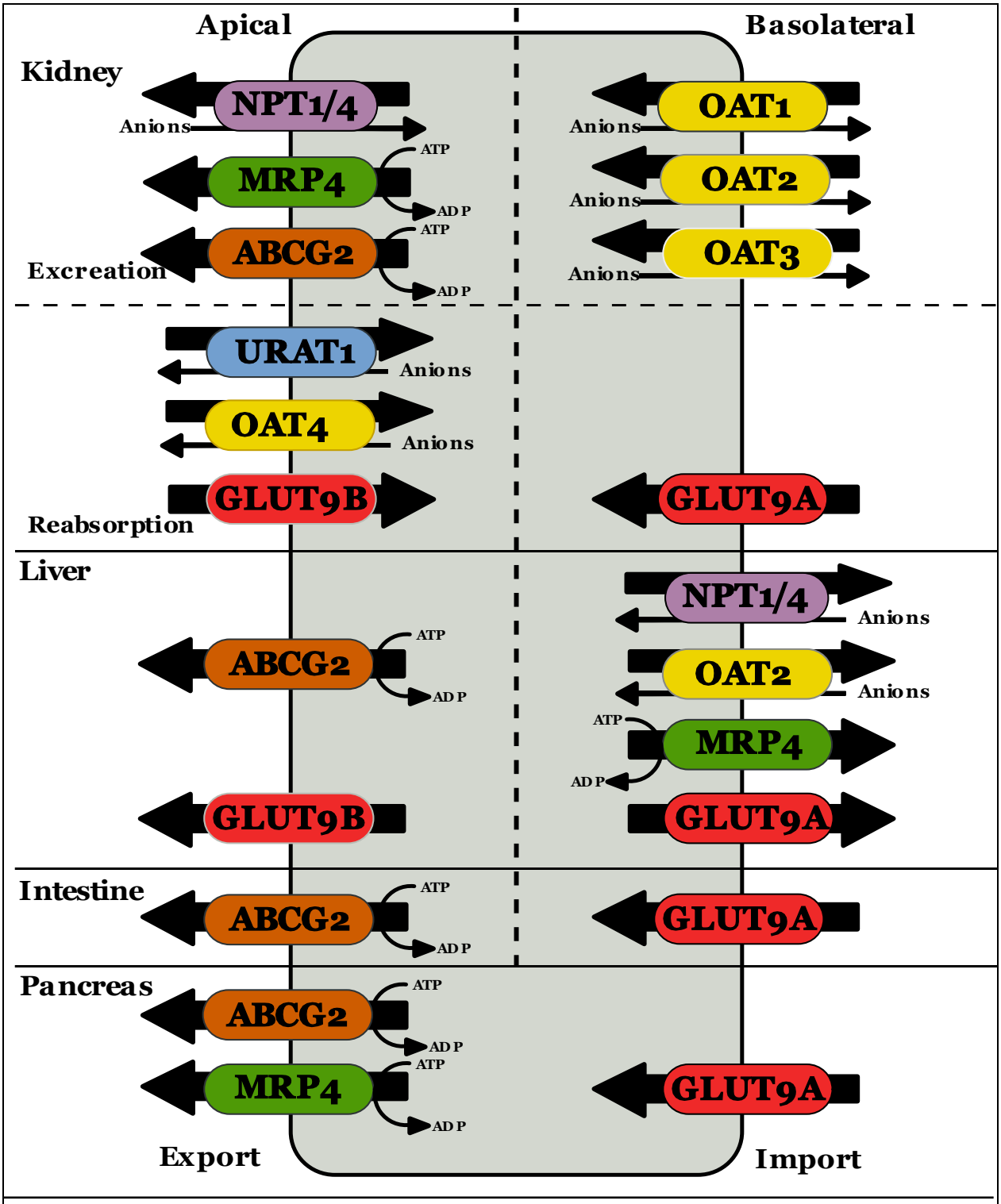

Figure 2. Uric acid transport.
Illustration of the arrangement of key uric acid transporters in different tissues.
The kidney is the major regulator of serum uric acid balance as a result of the balance between secretion and reabsorption. The liver is the major source of uric acid synthesis within the body but facilitates an alternative form of uric acid secretion through incorporation into the bile as it passes through the intestine. The pancreas provides an example of how other cells throughout the body may handle uric acid. It is based on observations made in our previous work.

1.2 The pancreas

The vast majority of endocrine cells in the pancreatic islets are β-cells (~70%) (Wang *et al.*, 2013), which produce and secrete insulin in response to high plasma glucose concentrations. The high proportion of β-cells in the pancreas point to their crucial role as the primary glucose sensor in the human body. Optimal control of blood glucose levels depends on dynamic and responsive changes in insulin production and secretion by the pancreatic β-cells and their capacity for a large increase in secretion during feeding states. Unlike other cell types in the pancreas, such as α-cells, where the population of cells do not significantly change throughout life, the pancreatic β-cell population remains dynamic, depending on various factors such as age, body weight and metabolic status (Saisho *et al.*, 2013). It has been shown that β-cell mass increases significantly around milestones that herald large growth periods i.e. infancy and puberty. This observation coupled with the analysis that β-cell mass increases proportionally to body mass indicates that the individual cells have a finite capacity for insulin secretion and as such maintaining the appropriate cell mass is key to maintaining insulin secreting capacity to cope with large increases in demand that may occur in the fed state.

1.2.1 Diabetes mellitus

As soon as the function or viability of the β-cells is compromised, the body is unable to release the amount of insulin necessary for adequate glucose homeostasis leading to the development of diabetes mellitus (DM, (Johnson *et al.*, 2013)). DM is considered a global epidemic with over 400 million diagnosed people, translating into almost 10% of the adult population (Jiang *et al.*, 2012)(Rojnic Putarek *et al.*, 2015)(Schipf *et al.*, 2014). DM is defined as the inability to adequately regulate blood glucose through insulin secretion. DM as a metabolic disease, particularly

detrimental in regard to both patient morbidity and mortality. This is due to the fact that although the initial symptoms are easily regulated as the disease progresses, it can rapidly induce multiple severe comorbidities such as kidney failure (Thomas *et al.*, 2015), cardiovascular depression (Qiu *et al.*, 2015), and peripheral neuropathy (Papanas & Ziegler, 2015). The disruption to adequately control glucose homeostasis has a major impact on multiple vital pathways such as glycosylation and glycation which in turn can have disastrous flow of effects affecting the regulation of healthy cell function (Ohtsubo & Marth, 2006). This is further compounded by the fact that as the disease progresses the damage to insulin secretion and receptor pathways is irreversible. After a certain point, patients are reliant on pharmaceutical regulation of serum glucose which lacks the dynamic responsiveness necessary to completely prevent further degradation and periodical dysregulation of serum glucose. This brings us to the largest problem DM presents to society as a whole, once this disease progresses past a certain point, patients become highly dependent on medication to maintain healthy serum glucose levels. The consequences are two-pronged effects of often leaving patients with a lower quality of life (Frøisland *et al.*, 2013), and of putting large strain on medical resources as disease progression requires more intensive interventions as more detrimental co-morbidities arise (Chevreul *et al.*, 2014)(Huber *et al.*, 2014).

1.2.2 Type-1 diabetes mellitus

Type-1 diabetes mellitus (T1DM) is well established as an autoimmune disorder which results in the destruction of pancreatic β-cells. Development of T1DM is strongly influenced by a genetic component, with the majority of T1DM cases being diagnosed during childhood or early adulthood (Olmos *et al.*, 1988). However, there is an increasing prevalence of evidence to suggest the involvement of environmental factors in the development of T1DM. The best evidence to support this theory comes from studies involving identical twins in which one twin presents with T1DM, however, contrary to

what we would expect to see if this condition was driven purely by genetic factors, only between 30-50% of the twins both presented with T1DM. This fact strongly indicates the involvement of environmental factors and/or cues, in combination with genetic factors, however, the environmental cues remain elusive (Olmos *et al.*, 1988). The defining characteristic of T1DM is the chronic, progressive destruction of pancreatic β-cell mass by an auto-immune response resulting in the inability to secrete sufficient insulin but patients retain normal insulin sensitivity as insulin receptors throughout the body remain unaffected (Pipeleers *et al.*, 2008).

1.2.3 Type-2 diabetes mellitus

Type-2 diabetes mellitus (T2DM) is by far the most prevalent form representing over 90% of all DM cases, and its prevalence has reached epidemic proportions worldwide (Wu *et al.*, 2014). The exact cause of T2DM is insufficiently understood, however, there is an overwhelming consensus that the changes in the modern diet and lifestyle and the accompanying metabolic stress have been the key contributing factors in T2DM development (Low *et al.*, 2015). Despite the fact that the cause resulting in the development of T2DM may differ between patients, the ultimate hallmark of chronic hyperglycaemia in T2DM is known to be caused by the impaired insulin secretion and insulin resistance (Johnson *et al.*, 2013). The currently proposed model of T2DM pathogenesis is based on the initial development of peripheral insulin resistance which over time leads to down-regulation of insulin receptors, leading to increased insulin secretion to the detriment of pancreatic β-cell survival and functional capacity (Johnson *et al.*, 2013). T2DM is far harder to treat than T1DM as the resistance to insulin signalling makes using endogenous regulatory pathways for intervention more difficult. The most common form of treatment is to regulate initial glucose metabolism from dietary factors by altering glucose consumption within the diet or by altering glucose handling in the body through drugs such as metformin (Vijayakumar *et al.*, 2017). These existing treatments have shown to be effective when paired with dietary and lifestyle changes. However, they are most effective if T2DM

is detected in the early stages as the impact on the quality of life has resulted in poor adherence rates for treatments reducing the overall effectiveness of treatment.

1.3 Uric acid and Diabetes mellitus progression

Numerous studies have investigated the potential correlation between two of the world's rising dietary driven health complications, hyperuricemia and diabetes mellitus. Studies in both young and old populations spanning up to 15 years have found a significant increase in the risk of developing diabetes in patients presenting with hyperuricemia. These studies have gone as far as to suggest that hyperuricemia causes a 27% increase in risk of developing diabetes (Krishnan *et al.*, 2012; Musacchio *et al.*, 2016) and that 1 in 11 new cases of diabetes could be attributed to this (Krishnan *et al.*, 2013).

This correlation is further supported by the mechanisms of reduced cellular viability described within previous research looking into the effects of uric acid within other parts of the body. The main hallmarks of T2DM development and progression are loss of viable pancreatic β-cell mass and peripheral insulin resistance. Both these effects have been described in experiments performed by Shimodaira *et al.*, 2014, Spiga *et al.*, 2017, Li *et al.*, 2018, Jia *et al.*, 2013 in which they were either induced or exacerbated by hyperuricemic conditions. As shown in previous studies the increase in autophagy as a result of increased mTOR inhibition and pro-autophagy protein activation alone could easily explain the initial loss of pancreatic β-cell mass or provide a means for progressive loss as a result of chronic exposure. This observation when also paired with the observed decreases in insulin sensitivity in peripheral tissues as a result of the inflammation that may arise due to increased uric acid generated damage associated molecular pattern (DAMP) signalling provides a potential causal basis for the observed correlation between hyperuricemia and T2DM development.

1.4 mTOR

The mechanistic target of rapamycin (mTOR) protein complexes C1 and C2 are major cellular regulators of pathways involved in cell metabolism, growth, proliferation and survival (Saxton & Sabatini, 2017). Activation of mTORC1 via amino acids or growth factors facilitates protein, lipid and nucleotide synthesis and consequently cell growth, whereas an inhibition of mTORC1 as a consequence of cellular stress or just starvation induces autophagy, a process regulating turnover of proteins or organelles in order to generate energy for cell survival. A disturbance of this pathway can lead to cell death (Vergès & Cariou, 2015). The regulation of mTORC2 is only beginning to be discovered, but the available evidence seems to suggest that only growth factors directly regulate this complex. Recent findings have revealed novel important roles for mTORC2 in the phosphorylation of AGC kinase family members such as protein kinase C (see figure 3) (Cameron *et al.*, 2017).

Although these complexes have distinct and different targets their method through which they activate their targets is the same. This activation is achieved through the function of mTOR as a serine/threonine protein kinase which directly phosphorylates target proteins leading in most cases to the activation of downstream pathways (Varusai & Nguyen, 2018). As such, their function is largely defined by their interaction with a regulatory-associated protein of mTOR (RAPTOR) in the case of mTORC1 or rapamycin-insensitive companion of mammalian target of rapamycin (RICTOR) in the case of mTORC2. These proteins differentiate the complexes and regulate which target proteins they can interact with. A protein that binds and negatively regulates both mTOR complexes in a mutual relationship is DEP domain-containing mTOR-interacting protein or DEPTOR for short (Catena & Fanciulli, 2017). Due to the fact that the mTOR complexes are involved in major cell processes, which determine cell health and survival, the impact of DEPTOR

and the regulation of its turn-over via ubiquitination are currently hot topics in cancer and diabetic research (Catena & Fanciulli, 2017).

1.5 DEPTOR

DEPTOR is a product of the DEPDC6 gene which codes for a protein with tandem N-terminal DEP (Dishevelled, Egl-10, Pleckstrin) domains and a C-terminal PDZ (Postsynaptic density 95, Discs large, Zonula occludens-1) domain (Jemth & Gianni, 2007). Due to the lack of previous studies into the function of the DEPDC6 gene product, it was named DEPTOR in reference to its DEP domains and its specific interaction with the mTOR core unit. Experiments confirmed that the endogenous mTOR core unit was specifically co-immunoprecipitated with DEPTOR and was confirmed using both RAPTOR-based and RICTOR-based immunoprecipitations. These were used to confirm the binding of DEPTOR to both mTOR complexes as mTOR complexes are defined by their binding to RAPTOR in the case of mTORC1 and RICTOR in the case of mTORC2 (Fig. 3). Initial studies were performed to investigate if DEPTOR interacted with mTOR and/or mLST8, the only protein common to both mTORC1 and mTORC2. Reciprocal experiments showed that the PDZ domain of DEPTOR mediates its interaction with mTOR.

In terms of function, DEPTOR directly suppresses mTOR by interacting with the FAT domain of the mTOR core unit via a PDZ domain located at its C-terminus (Peterson *et al.*, 2009). It results in the inability of binding of key mTOR substrates resulting in functional inhibition of both mTOR complexes and consequently a reduction in cell metabolism, growth pathways and proliferation pathways. It is coupled with the upregulation of autophagic activity resulting in large scale suppression of cellular energy demand, function and viability. This leads to its role in disease pathology which has focused on cancer. In this case, most studies have shown the major decrease in DEPTOR expression leads to increased rates of tumour growth and survivability in breast,

pancreatic, and prostate cancers, however, this trend is reversed in thyroid cancers (Catena & Fanciulli, 2017). This difference between different cancers is explained as being a result of a proposed protection form endoplasmic reticulum stress in these cells as only cells characterised with high protein synthesis and expression show this inverse response to DEPTOR (Catena & Fanciulli, 2017). Additionally, DEPTOR is thought to act as a key metabolic regulator as it has been shown that within the liver it functions to accelerate the shift towards a fasting response when the body is put under starvation conditions. DEPTOR's proposed function further promotes the idea that DEPTOR is a low energy state driven protein synthesis and cell growth regulator (Caron *et al.*, 2017).

This feeds into the understanding of the regulation of DEPTOR. According to the current understanding, DEPTOR and the mTOR complexes are engaged in a dynamic inhibition loop in which DEPTOR is both able to inhibit the mTOR complexes but is also inhibited by them as illustrated in figure 3. Although the finer details what determines the directionality is unclear, the current understanding indicates extracellular environmental factors dictate the stability of DEPTOR and the rate at which it is degraded as a result of ubiquitin signalling. An explanation is provided by the previous observations, why DEPTOR activity is greatest under starvation or low energy conditions as this would allow for the body to down-regulate energy demand by down-regulating the mTOR complexes. Hence, DEPTOR presents as a prime candidate for my study as it provides a potential link between the changes we see in the cellular environment in conditions like hyperuricemia and DM.

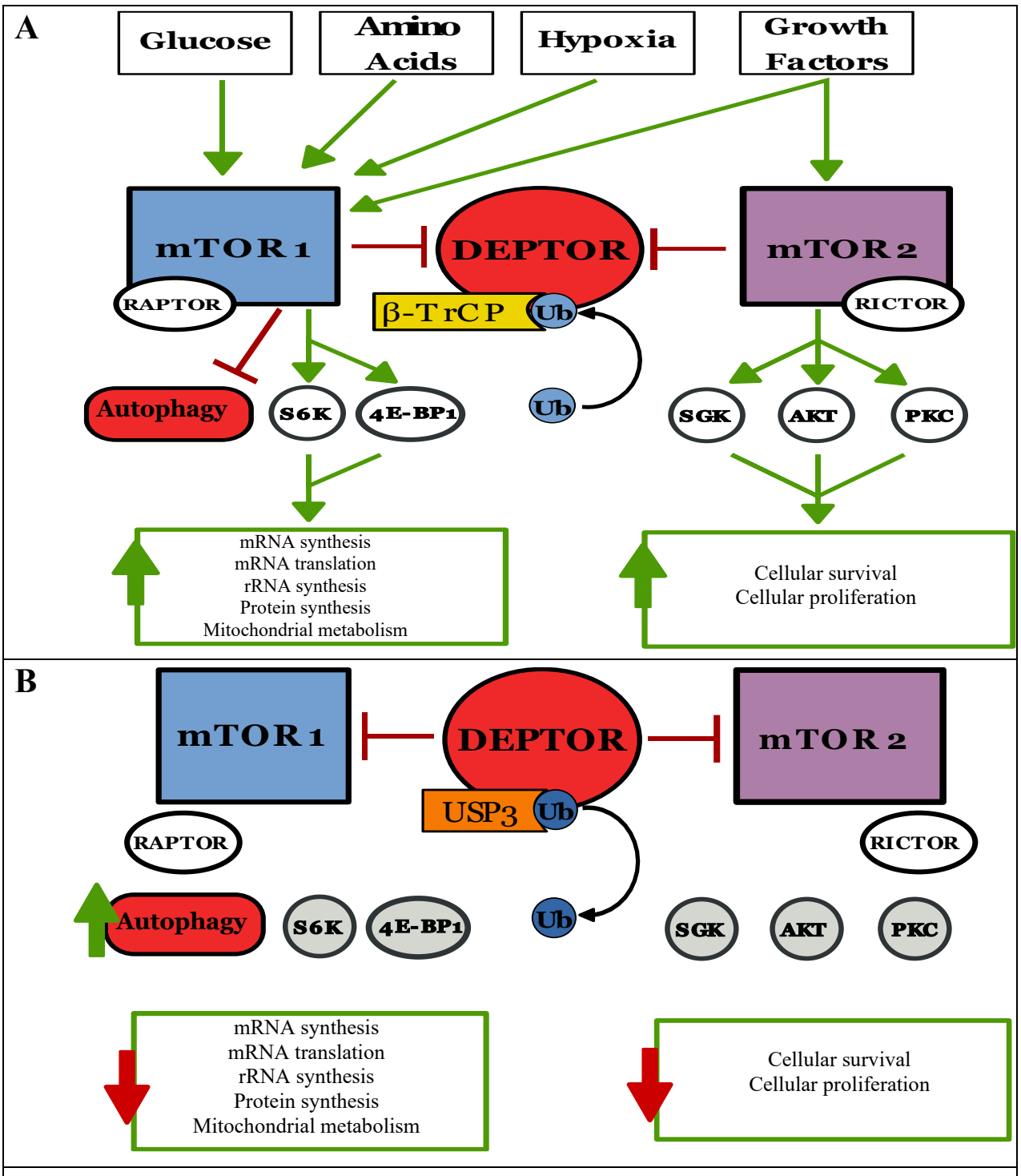

Figure 3. A. mTOR function under normal conditions. B. Proposed uric acid driven DEPTOR activation.

(A) This figure shows the known function of the mTOR complexes under physiological normal conditions. Through their activation due to multiple nutrient based factors the mTOR complexes are responsible for the phosphorylation and activation of multiple substrates that are key for the maintenance of several cellular functions. **(B)** A proposed model for the activation of DEPTOR by uric acid is illustrated. Under these conditions, we propose that the increase in serum uric acid leads to increased DEPTOR stability. This inhibits the function of the mTOR complexes and leads to alteration in cellular function as a consequence.

1.6 Ubiquitination of proteins and DEPTOR

Ubiquitination is a post-translational protein modification which determines the fate/degradation of proteins via the proteasomal pathway (Heideker & Wertz, 2015). It is dependent on the interaction between two processes, the ubiquitination and deubiquitination facilitated by respective enzymes. The ubiquitination cascade has three major components: the first component is E1 or ubiquitin activating enzyme. E1 is responsible for the binding of free ubiquitin which is bound to E1 along with ATP activating ubiquitin (Neutzner & Neutzner, 2012). Following this, E1 transfers the bound ubiquitin to E2 or ubiquitin conjugating protein (Zhang & Sidhu, 2014). E2 then carries the ubiquitin until it binds to E3 or ubiquitin ligase. The E3 ligase is the most specific of the three components of the ubiquitination cascade and is responsible for binding to specific target proteins. It transfers the ubiquitin from E2 to the target protein resulting in ubiquitin-tagging of the protein and the degradation or trafficking of the target protein (Berndsen & Wolberger, 2014). Because E3 ligases are the most specific component of the ubiquitination cascade they provide the best target for treatment as their specificity reduces the potential of off target effects and interference due to unexpected alterations of non-target proteins.

This specificity arises due to the interactions between unique binding sites found on an E3 ligase and the corresponding domain on a target protein. This also allows for a temporal sequence as this binding site may be internalised within the protein's folding structure until the addition of a posttranslational modification leads to a conformational change in protein folding allowing for interactions with a respective E3 ligase. It should also be noted that there are different types of ubiquitination varying based on the number of bound ubiquitin and their arrangement leading to mono- or polyubiquitination. This difference in number and arrangement allows for multiple possible ubiquitin signals and is one of the underpinning principles in the ideas regarding

ubiquitin's role as a multi-destination protein trafficking signal. As this process is dependent on the specific interaction between a protein and its E3 ligase this process can be disturbed through either the addition of post-translational modifications that prevent the externalisation or actively internalise the domains necessary for recognition and interaction with an E3 ligase or through reduction in the availability of the ligase itself (Liu *et al.*, 2015).

In addition to this, as we discussed the number and distribution of bound ubiquitin is also key to regulating the consequences of ubiquitination, as such anything that would reduce the number of or change the arrangement of the bound ubiquitin in a polyubiquitin chain would have massive impacts on the proteins turnover or trafficking (Ohtake *et al.*, 2015). Ways in which this may occur include the limitation of available ubiquitin or through the addition of molecules to the bound ubiquitin that modify the ubiquitin chain structure by either altering the bond structure or through simply premature termination of a polyubiquitin chain such as the process of acetylation (Ohtake *et al.*, 2015). To investigate uric acid's role as a potential modulator of this process, we will be examining DEPTOR's E3 ligase, beta-transducin repeat containing protein (β-TrCP). This would explain previously observed changes to DEPTOR stability as inhibition of an E3 ligase would result in the reduction of protein degradation (Zhao *et al.*, 2005).

1.6.1 β-TrCP

We have chosen to focus on beta-transducin repeat containing protein (β-TrCP) as this is the known E3 ligase of DEPTOR (Zhao *et al.*, 2005), and as such any alteration to its expression would have a direct impact on DEPTOR ubiquitination resulting in changes in protein levels.

β-TrCP belongs to the F-box family of proteins, which forms a multicomponent Skp1/Cul1/F-box protein (SCF) ubiquitin ligase complex with the β-TrCP complex functioning as the target recognition subunit. As a general role β-TrCP functions to regulate cell survival and turnover rates

thought regulating the turnover of key proteins. Examples of these proteins include nuclear factor (erythroid-derived 2)-like 2 (Nrf2), NF-κB, and mammalian period-1 protein (PER1). Nrf2 controls the expression of genes that participate in biotransformation reactions, redox homeostasis, energetic metabolism, DNA repair, and proteostasis (Cuadrado, 2015). NF-κB, as stated previously, is key to immune and inflammation response and is controlled by ubiquitination via β -TrCP (Melikian *et al.*, 2017). Additionally, PER1 is a key clock gene responsible for maintaining circadian rhythm (Yang *et al.*, 2009), and as a consequence of this regulates mild fluctuations in full body metabolic process. These are just some of a growing list of identified downstream β-TrCP ubiquitin substrates, implicating a critical role for β-TrCP in regulating both, cell cycle progression and cellular survival.

β-TrCP as the ubiquitin ligase for DEPTOR works by ubiquitinating DEPTOR in the c-terminus domain. This ubiquitination is triggered in response to the phosphorylation of DEPTOR at Ser293 and Ser299 by the mTOR complexes. This has been confirmed through the use of β-TrCP siRNA and targeted DEPTOR point mutations, both of which confirmed that when β-TrCP expression or binding was inhibited DEPTOR became more stable leading to reduced mTOR function and reduced activation of downstream mTOR pathways (Zhao *et al.*, 2005).

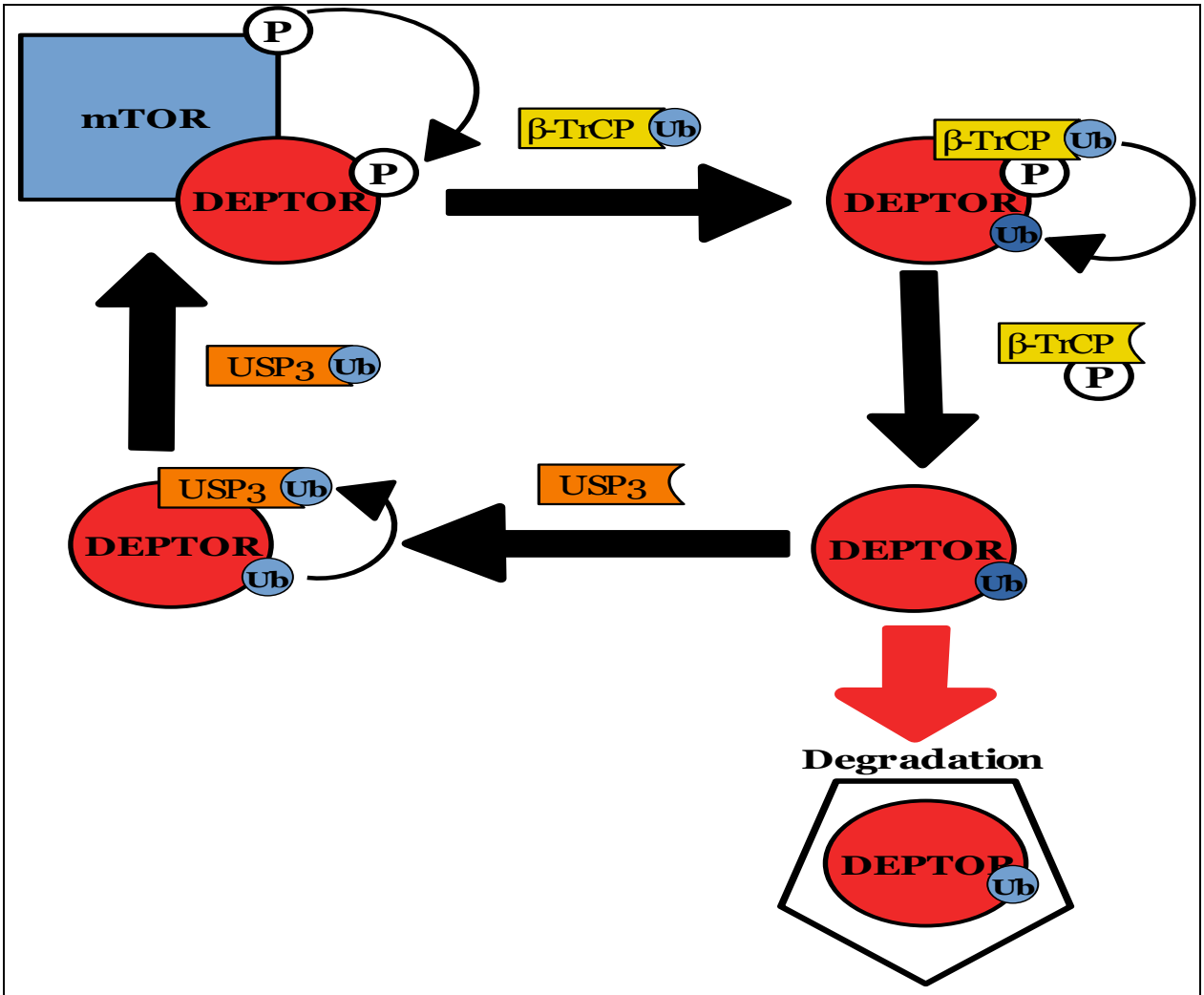

Figure 4. DEPTOR regulation via mTOR.
This figure shows how DEPTOR is phosphorylated by mTOR leading to β-TrCP-mediated ubiquitination and potential degradation which may be prevented by deubiquitination facilitated by USP3.

1.7 De-ubiquitination

The counter to the ubiquitination cascade is the activity of deubiquitinating enzymes, DUBs also called ubiquitin specific proteases (USPs). There are two main classes of DUBs/USPs, cysteine proteases and metalloproteases. Although these two classes achieve this differently, the primary function of a DUB/USP is to cleave the peptide bond between ubiquitin and the protein it is bound to thus removing the ubiquitin from the protein and preventing its degradation (Heideker & Wertz,

2015). USP's function through cleavage of the isopeptide bond at C-terminal glycine residues of ubiquitin. These ubiquitinyl bonds can be generated at the N-terminus of another ubiquitin molecule, the side chain of lysine in another ubiquitin molecule or to the side chain of a lysine residue in another protein (Heideker & Wertz, 2015).

Despite a strong homology observed between USP, recent three-dimensional structural imaging of several USPs reveal striking differences in the accessibility to the catalytic pocket pointing to potentially high specificity (Daviet & Colland, 2008). Although the key DUB/USP for DEPTOR has yet to be confirmed, initial studies have demonstrated that the action of deubiquitinases including ovarian tumour domain-containing ubiquitin aldehyde-binding protein 1 (OTUB1) and Ubiquitin carboxyl-terminal hydrolase isozyme L1 (UCHL1) can lead to alterations in DEPTOR expression, and that this is significant enough to alter the regulation of mTOR (Zhao *et al.*, 2018). Due to the fact that alterations of the expression of a DUB have a large impact on protein function any potential DUB cannot be ignored.

1.7.1 USP3

Recent studies have shown some potential candidates for a DEPTOR deubiquitinase. These studies have shown multiple potential deubiquitinases interact with DEPTOR indicating that they may have different functions (Zhao *et al.*, 2018). This difference in function is most likely due to having different activation conditions or pathways. However, when we began this study the work by Zhao and co-workers had yet to be released. As such the selection of the Ubiquitin specific protease 3 (USP3) was made based on the fact that it is highly expressed in the pancreas (Santin *et al*., 2012; Gorelik & Sido, 2017) and has been shown to be involved in diabetic neuropathy in multiple regions in the body (*Goru et al*., 2017). This combined with the fact that USPs can not only remove all protein bound ubiquitin but also degrade polyubiquitin chains means that any changes in USP3

expression could lead to changes in DEPTOR degradation. This could occur through the complete removal of ubiquitin bound to DEPTOR, or through significant degradation of any polyubiquitin chains preventing the transport of DEPTOR to the proteolysosome for degradation via proteolysis (Fig. 4).

1.8 Autophagy

Autophagy is the process by which the cell breaks down damaged proteins, misfolded proteins, damaged organelles or certain overexpressed proteins to provide additional energy. In healthy cells, this process is tightly controlled, and in addition to providing energy, it also functions to remove enzymatic or regulatory proteins that are overexpressed for current cell function (Ravanan *et al.*, 2017). Autophagy can take place as a result of many pathways, however, they can largely be defined and categorised as microautophagy which involves the incorporation of small regions of the cytosol into a lysosome degrading small soluble proteins distributed within the cytosol. Chaperone mediated autophagy (CMA) which uses specific chaperone molecules to transport specific single proteins to digestive vesicles. Macroautophagy involves the enveloping of targets in a double membrane which is then fused with lysosomes to form an autolysosome. Macroautophagy targets larger proteins, insoluble proteins and organelles. Although all of these forms of autophagy have different targets, they are all largely responsive to the same triggers being starvation or cellular stress. These pathways are active in cells under non-stress conditions as they provide the necessary degradation to maintain healthy protein turnover by removing damaged or decayed proteins (Takahiro Shintani & Klionsky, 2004).

Although all types of autophagy are important, this study be will focusing on macroautophagy for two reasons: Firstly, out of all the types of autophagy macroautophagy has the greatest potential impact for change while still being easy to measure. This is due to the fact that microautophagy

has a lower impact at equal levels of activity and CMA has a high degree of specificity making it more difficult to take general measurements in change of activity. Secondly, macroautophagy is regulated by mTOR, and this is due to the fact that multiple autophagy regulating pathways are controlled at some level by mTORC1 including, phosphoinositide 3-kinase (PI3K) which is important for target recognition and Unc-51 like autophagy activating kinase (ULK1/2) which is responsible for signalling the initiation of autophagic vesicle formation (Sheng *et al.*, 2017). Following the signalling from ULK1/2, the formation of the autolysosome is regulated by several proteins including microtubule-associated proteins 1A/1B light chain 3B (LC3 II). LC3 functions both as a regulator of autophagosome formation but also as a marker of autophagosome maturation (Huang & Liu, 2015).

Although autophagy is necessary for the normal function of a cell if it becomes disturbed it can lead to massive loss of function as excessive protein degradation results in the disruption of key protein cascades. If autophagy is not brought back to healthy levels within a sufficient timeframe the effects of excessive protein degradation can trigger programmed cell death or apoptosis (Lõpez De Figueroa *et al.*, 2015).

1.9 Aims and research objectives

The aim of this study was to determine the involvement of the mTOR complexes in the loss of pancreatic β-cell mass under hyperuricemic conditions via the regulation of DEPTOR.

To determine the exact mechanism, how uric acid regulates DEPTOR turn-over, we will examine whether hyperuricemic conditions induce any changes in DEPTOR ubiquitination, which is a hypothesis based on previous results. A change in ubiquitination of DEPTOR can have several reasons: **1)** a change in the DEPTOR-specific ubiquitin ligase expression, namely E3 ubiquitin

ligase β-TrCP; **2)** a change in the ubiquitin specific protease, possibly USP3, expression; **3)** by direct modification of DEPTOR by uric acid.

1.9.1 Hypothesis

We hypothesise that hyperuricemia reduces the ubiquitination of DEPTOR and that a change in expression of the E3 ubiquitin ligase β-TrCP or the deubiquitinase USP3 is responsible for this change of DEPTOR ubiquitination. Furthermore, we hypothesise DEPTOR not to be modified directly by uric acid. As a result of this activation of DEPTOR, the subsequent inhibition of mTOR complexes will result in reduced cell viability of pancreatic β-cells and increased autophagy.

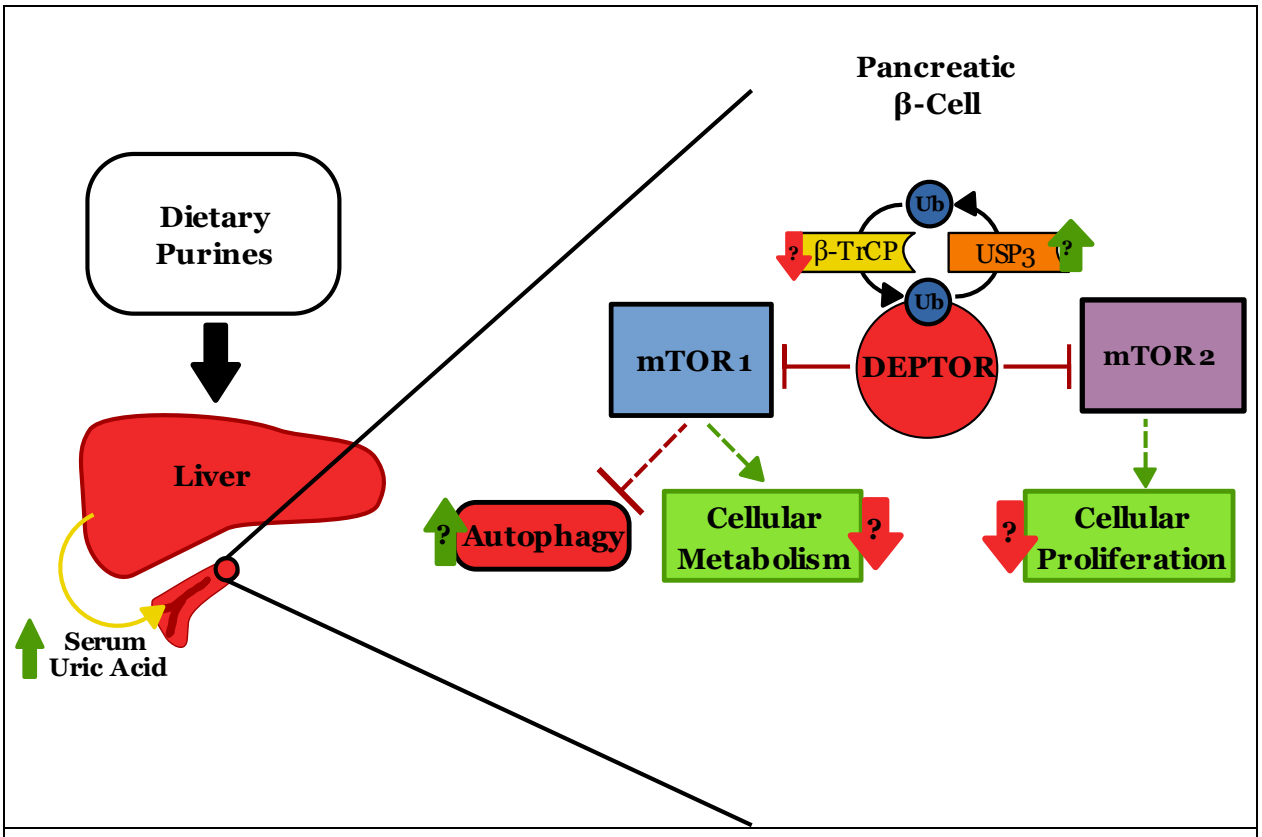

FIGURE 5. Hypothetic Model.
Increased serum uric acid as a result of increased dietary purines alters DEPTOR ubiquitination within pancreatic β-cells. This leads to a loss in cell viability due to decreases in cellular metabolism and growth and increases in cellular autophagy as a result of changes to mTOR activity. This change in mTOR activity is the result of changes in DEPTOR ubiquitination.

Methods

2.1 Cell lines

2.1.1 Human 1.1B4 cells

1.1B4 is an immortalised hybrid cell line formed by the electrofusion of a primary culture of human pancreatic islet cells with human ductal carcinoma cells. 1.1B4 cells were used as an alternative functional model of a human pancreatic β-cell, due to the low availability of human primary cells. Furthermore, functional assessments have shown 1.1B4 cells exhibit a similar cellular response and changes in gene expression, in response to varying extracellular glucose concentrations, to primary pancreatic islets (McCluskey *et al.*, 2011). 1.1B4 cell line was used as a human cell model of a pancreatic β-cell, allowing the results of this study to be more relatable in terms of studying the component of hyperuricemia in human type-2 diabetes mellitus development.

2.1.2 Mouse MIN6 cells

MIN6 cells originate from a transgenic C57BL/6 mouse insulinoma expressing an insulin-promoter/T-antigen construct. They form islet-like cells. MIN6 cells express GLUT-2 and glucokinase and respond to glucose within the physiological range (Miyazaki et al., 1990). They are used regularly throughout contemporary literature and are the most common mouse cell line used in the research of diabetes when a mouse model is required.

2.2 Cell Culture, Harvest and Treatment

2.2.1 Cell culture

2.2.1.1 1.1B4 culture

1.1B4 cells were cultured and maintained in Roswell Park Memorial Institute medium (RPMI-1640, *SIGMA*®) with 11mmol/L glucose, 10% FBS, 100U/mL penicillin G sodium, 100µg/mL

streptomycin sulfate at 37°C and 5% CO_2. The medium was supplemented with 2g/L $NaHCO_3$ and brought to a pH of 7.4. Passages 30-70 were used for all cellular experiments. Cell lines were passaged once a confluence of approximately 85% or greater was achieved by washing with phosphate-buffered saline (PBS: 137mM NaCl, 2mM KCl, 10mM Na_2HPO_4 and 1.8mM KH_2PO_4) prior to detachment with 0.25% (w/v) trypsin (TrypLE™ express; *life technologies*®) and splitting at a 1:10 ratio.

2.2.1.2 MIN6 culture

Mouse insulinoma (MIN6) cells were cultured and maintained in Dulbecco's modified eagle's medium – high glucose (SIGMA®), 10% FBS, 100U/mL penicillin G sodium, 100µg/mL streptomycin sulfate at 37°C and 5% CO_2. The medium was supplemented with 3.4g/L $NaHCO_3$, 5µL/L of β-mercaptoethanol and brought to a pH of 7.4. Cell lines were passaged once a confluence of approximately 80% or greater was achieved by washing with phosphate-buffered saline (PBS: 137mM NaCl, 2mM KCl, 10mM Na_2HPO_4 and 1.8mM KH_2PO_4) prior to detachment with 0.25% (w/v) trypsin (TrypLE™ express; *life technologies*®) and splitting at a 1:5 ratio.

2.2.2 Treatment

2.2.2.1 Uric acid stock solution

A uric acid stock solution was prepared at the concentration of 5mM, dissolving uric acid sodium salt (*SIGMA*®) in 1M sodium hydroxide (NaOH), brought to a pH of 7.4 using 1M hydrochloric acid (HCl) and final volume was adjusted using PBS.

2.2.2.2 Generation of samples

For the generation of cell samples for co-immunoprecipitation and western blotting, 1.1B4 and MIN6 cells were harvested when they reached greater than 80% confluence in a 25cm^2 flask. Cells were then seeded into 6-well plates at a density of 1x10^4 for 1.1.B4 and 5x10^4 for MIN6 cells. Cells were incubated in their respective medium for 24 hours prior to any treatment to allow cell adhesion. Cells were cultured for an additional 72 hours in their respective conditions. 300μM uric acid represents a physiologically normal condition for 1.1B4 cells, while 500μM represents a hyperuricemic condition, with an additional flask of cells left untreated to act as a control.

2.2.3 Harvesting of cell samples

Following 72 hours of treatment, all medium from each well was aspirated and the cells in each well were washed in sterile PBS to remove any dead cell debris and trace of compounds used during conditioning.

2.3 Protein analysis

2.3.1 Extraction of protein for western blot analysis

To facilitate the analysis of the expression of our target proteins the total cellular protein had to be extracted from the cultured and treated cells. To minimise any protein degradation, the protein was extracted directly from 6-well plates containing the treated cells. To lyse the cells and liberate the protein the cells were bathed in 100μL of radioimmunoprecipitation (RIPA) buffer, containing a protease inhibitor cocktail (*ThermoFisher Scientific*™). The resulting lysate was collected into a 2mL Eppendorf tube and centrifuged at 13,000 rpm for 5 minutes at 4°C to ensure maximal separation of cell debris and proteins solution. The supernatant containing the protein extract was transferred to a fresh Eppendorf tube. Following this, the extracted protein concentration was

measured against a known BSA (bovine serum albumin) standard using *Bio-Rad* DC™ protein assay (*Bio-Rad*®) and then stored at -20°C until needed.

2.3.2 Extraction of protein for Co-immunoprecipitation analysis

To allow us to detect the changes in DEPTOR bound proteins a co-immunoprecipitation is required. To facilitate this, proteins were extracted from treated cells in a way to maintain as accurate representation of protein to protein bonds as possible. To this end the treated cells as obtained in section **2.2.3** were bathed in 100µL of a specialised, preheated PBS based lysis buffer, containing 1% SDS and 10µM carbobenzoxy-Leu-Leu-leucinal (MG-123, *Sigma-Aldrich*) which is a proteasome inhibitor that has been shown to improve the preservation of protein ubiquitination. This mix was then passed 5-times through a 22-gauge needle and diluted with an equal volume of a TBS + 0.4% Triton X-100 to ensure a constant viscosity that would be suitable for the later stages of co-immunoprecipitation. This lysate was then immediately measured against a known BSA standard using *Bio-Rad* DC™ protein assay (*Bio-Rad*®) to determine its concertation; after this, the protein extract was immediately subjected to the protein isolation procedure outlined below.

2.3.3 Target protein isolation

To isolate the target protein (DEPTOR) from the total protein extract the target protein must be marked and separated from all other proteins present. This was achieved by first incubating 100µg of whole cell protein with 2µL of a mouse based DEPTOR antibody (ab103298**)** for 2 hours at room temperature on a shaker table. This allowed the antibody to bind to the target protein providing a means by which to isolate it from the total protein extract. Following this, 30µL of IgG sepharose protein beads (*Sigma-Aldrich*) and left to incubate for 1 hour at room temperature on a shaker table. This provides a matrix for the antibody-bound DETPOR to anchor itself to during the

removal of the remaining total protein extract. Once this is completed, any unbound proteins are washed away from the IgG beads using a 4 x PBS washes leaving only the bound DEPTOR remaining. Finally, to release the bound DEPTOR from the IgG beads 30µL of 5 x loading buffer (0.25% bromophenol blue, 0.5 M DTT, 50% glycerol and 10% Tris-HCl) was added to the beads and the sample was heated at 95°C for 5 minutes and afterwards used for gel electrophoresis as outlined below.

2.3.4 Gel-electrophoresis and membrane transfer

To image the levels of protein, proteins need to be separated by weight to allow for the visualisation of different proteins. This is the same for both the standard western blot and the co-immunoprecipitation which was achieved using the method below. In the case of the western blot 10µL of 5 x loading buffer (0.25% bromophenol blue, 0.5M DTT, 50% glycerol and 10% Tris-HCl) was added to 100µg protein of the protein samples that we created in **2.3.1,** these were incubated at room temperature for 5 minutes. Samples were then loaded onto a 12% SDS-PAGE (SDS-Polyacrylamide Gel Electrophoresis) gel. For molecular weight estimation, 7µL of Precision Plus Protein™ standard (*Bio-Rad*®) was loaded into the first well of the gel which was then run at 120V for 90 minutes.

To allow for the proteins to be detected, they need to be exposed to antibodies. As a means to facilitate this, the proteins were transferred from the gel to a PVDF membrane (*Immobilon*®) using a 'semi-wet' transfer protocol which entailed sandwiching the gel and the membrane between four layers of in transfer buffer (25mM Tris, 192mM glycine, 20% v/v methanol and pH ~8.3) saturated filter paper and being exposed to a directional current of 25V and 1.2A for 30 minutes using the turbo blotting system (*Bio-Rad*®).

Once the proteins were transferred onto the membrane, a 5% non-fat milk blocking buffer (5% non-fat milk powder in PBST) was introduced for 1 hour at room temperature whilst the blocking buffer and membrane were agitated by a shaker table. In the case of the co-immunoprecipitation, the same steps as above were used with the exception of the addition of 10µL of 5 x loading buffer (0.25% bromophenol blue, 0.5 M DTT, 50% glycerol and 10% Tris-HCl) as the appropriate amount of loading dye had already been added as a part of the protein isolation preparation described in **2.3.3.**

2.3.5 Protein detection and imaging of the membrane

To detect our target proteins, the membranes on which we had transferred our proteins onto were first exposed to a target specific antibody and then incubated overnight at 4°C on a tilt table, the concentrations for these antibodies can be seen below in table 1. Following this, the blots were washed four times for 10 minutes in PBST to remove any unbound primary antibody; then they were incubated in secondary antibody for 1 hour at room temperature on a shaker table. Once this had been completed, the blots were washed two-times in PBST for 10 minutes and two times for ten minutes in PBS to remove excess secondary antibody. Following this, the blots were imaged using the Syngene Pxi4 (*Integrated Scientific Solutions Inc*.) imaging system to detect the fluorescence of the secondary antibodies. Once the target was imaged, the blot was then stripped using a mild stripping buffer (15g glycine,1g SDS, 10mL Tween20, pH 2.2) and re-imaged to confirm that the previous signal was removed. Following this, the membranes were reincubated with the primary antibodies that were used to detect the proteins being used as loading controls, DEPTOR, for the co-immunoprecipitation and GAPDH for the western blots. It should be noted that in the case of the co-immunoprecipitations both ubiquitin and uric acid were imaged on the same blot as the difference in secondary antibody means that they could be determined by the use

of a specific stimulus frequency thus reducing the need to strip the blot an additional time with the hopes that this will help to preserve the more delicate signal of the bound proteins.

2.3.6 Western blot analysis

Once the blots had been imaged the resulting bands of fluorescent response were analysed using the software Image J (*National Institutes of Health and the Laboratory for Optical and Computational Instrumentation*). This system analyses the intensity of the bands using relative area density (RAD) to generate a numerical representation of the expression. This was then used to calculate the relative expression of proteins. In the case of the western blot data, the data was normalised to the untreated cells first as this provides a common denominator between the two cell types, then these ratios were corrected based on how the GAPDH values of the treated cell groups differed from the untreated cells so as to normalise against any shift that may be due to errors in protein loading.

In the case of the co-immunoprecipitations, the math that produced the expression ratios was the same but DEPTOR was used to normalise instead of GAPDH because first there was no GAPDH to measure, second as DEPTOR was the TARGET of the co-immunoprecipitation. Using DEPTOR as a loading control ensured that we have equal amounts of DEPTOR present to ensure an accurate representation.

Table 1. Target antibody conditions.

Conditions used to detect the target proteins of interest. M = mouse, G = goat, Rb = rabbit, Ch = chicken.

Target	Primary antibody	Concentration	Incubation time	Brand ID	Required secondary antibody	Secondary concentration	Incubation time	Brand ID
USP3	Rb α USP3	1 :1,000	overnight	ab101473	G α Rb	1: 10,000	1 hour	SA5-10036
β- TrCP	M α β-TrCP	1 :500	overnight	sc-390629	G α M	1: 5,000	1 hour	35518
DEPTOR	Rb α DEPTOR	1 :1,000	overnight	ab103298	G α Rb	1: 10,000	1 hour	SA5-10036

GAPDH	Ch α GAPDH	1 :1,000	overnight	ab83956	G α Ch	1: 10,000	1 hour	ab175779
Ubiquitin	M α Ubiquitin	1 :1,000	overnight	sc-8017	G α M	1: 5,000	1 hour	35518
Uric Acid	Rb α Uric Acid	1: 1,000	overnight	ab53000	G α Rb	1: 10,000	1 hour	SA5-10036

2.4 Live cell viability

2.4.1 Cellular metabolism

MTT assay is a colorimetric assay for assessing the cells' metabolic activity and quantification of the relative viability of cells. Intracellular mitochondria exhibit NADH-dependent cellular oxidoreductase enzyme, which reduces the tetrazolium dye MTT (3-(4, 5-dimethylthiazol-2-yl)-2, 5-diphenyltetrazolium bromide) to insoluble, purple formazan. By solubilising and measuring the amount of formazan, this allows the relative quantification of the number of viable, proliferative cells, as cytotoxic cells undergoing cell death or cytostatic cells that are less proliferative express lower amounts of functional mitochondria that exhibit the NADH-dependent cellular oxidoreductase enzyme.

For MTT assays, 1.1B4 and MIN6 cells were harvested when flasks reached 80% confluence or greater and were seeded onto 96-well plates at 2 x10^4 cells per well. After this, cells were incubated for 72 hours with 300μM uric acid representing a physiologically normal condition, and 500μM representing a hyperuricemic condition, with wells of cells left untreated to act as a control. Following treatment with their appropriate conditions, media was aspirated and 100μL of fresh media was added. In addition to this, 10μL/well of 5mg/mL MTT solution (final MTT concentration of 0.5mg/mL) was added and the cells were incubated for 4 hours at 37°C. Following incubation, 85μL/well of MTT solution was removed and 50μL/well of DMSO was added to dissolve the formazan crystals produced by mitochondrial respiration. DMSO in each well was thoroughly mixed by repeated pipetting and then the plate was incubated for an additional 20

minutes at 37°C. Dissolved formazan in each well was quantified via absorbance values measured at 540nm with a *BioTek*® Synergy 2 multi-mode microplate reader.

2.4.2 Autophagy Assay

Autophagy Detection Kit (ab139484) measures autophagic vacuoles and monitors autophagic flux in live cells by using a cationic amphiphilic tracer (CAT) dye that rapidly partitions into cells labelling of vacuoles associated with the autophagy pathway.

1.1B4 and MIN6 cells were harvested when flasks reached 80% confluence or greater and were seeded onto 96-well plates at 2 $x10^4$ cells per well. After this, cells were incubated for 72 hours with 300μM or 500μM uric acid with wells of cells left untreated to act as a control. After this, the culture media was aspirated, the cells were washed with an assay buffer and then exposed to a dual detection mix consisting of the CAT dye and a dye designed to detect healthy cell nuclei. The cells were then incubated in the dark at 37°C for 30 minutes after which the detection mix was removed, and the cells were washed again with assay buffer. Following this, the level of autophagy and cell nuclei were determined through quantification of their respective fluorescent dyes. CAT dye produced fluorescence in each well was quantified via fluorescence values measured with an excitation/emission spectrum of 480/550nm, and nuclei were determined using excitation/emission 350/462nm. Both were determined using a *Molecular Devices*® SpectraMax i3x multimode detection microplate reader.

2.4.3 Apoptosis Assay

The apoptosis assay is performed using the Abcam apoptosis/necrosis detection kit (ab176749). This uses three different dyes to quantify necrosis, apoptosis and healthy cells. It achieves this by taking advantage of the differing nature of the cellular processes. For apoptosis, the dye used in the

kit fluoresces upon binding to phosphatidylserine (PS). Under normal conditions, PS is stored within the cell until apoptosis begins at which point it is transferred to the cell membrane. As the dye used to detect apoptosis cannot enter the cell all the fluorescence that is generated by the dye only arises due to apoptotic expression of PS on the cell surface. In the case of necrosis, the kit uses a dye that only fluoresces when it encounters proteins that are only expressed within the nucleus. Because this dye cannot cross the membrane any fluorescence that arises due to that dye is because of loss of membrane integrity that is consistent with necrosis or late stage apoptosis.

1.1B4 and MIN6 cells were harvested when the flasks reached 80% confluence or greater and were seeded onto 96-well plates at $2x10^4$ cells per well. After this, cells were incubated for 72 hours with 300μM or 500μM uric acid with wells of cells left untreated to act as a control. Then, the culture media was aspirated, the cells were washed with assay buffer. Then, exposed to a detection mix consisting of Phosphatidylserine (PS), the kits chosen marker for early stage apoptosis, 7-aminoactinomycin D (7-AAD) a membrane impermeable dye that marks late stage apoptosis, and CytoCalcein Violet 450 which detects live cells. The cells are then incubated in this detection mix for 30 minutes at 37°C while being protected from light to preserve the function of the fluorescent dyes. After this, the detection mix is removed and the cells are washed to remove any unbound dye. The dyes were then quantified using a *Molecular Devices*® SpectraMax i3x multimode detection microplate reader with the excitation/emission values of 490/525nm for PS, 550/650nm for 7-AAD and 405/450nm for CytoCalcein.

2.5 RNA analysis

2.5.1 Extraction of total RNA

To analyse the expression of deubiquitinase RNA we first need to extract the cellular total RNA. 1.1B4 cells were grown as previously described and total RNA was extracted using the

NucleoSpin® miRNA kit (*Macherey-Nagel*™). The extraction was performed according to the manufacturer's protocol and the total RNA was eluted with 50µL of RNase free water. RNA concentration and purity were assessed using the Take-3 plate on a *BioTek*® Synergy 2 multi-mode microplate reader (*Millennium Science*™) with the target being concentration and purity exceeding 500ng/mL and 90%, respectively. Samples were stored at -20°C until needed.

2.5.2 Reverse transcription

To allow for the gene expression to be measured using qPCR the RNA must first be converted to cDNA. This was done using PrimeScript™ RT reagent kit (*Takara*®), adhering to manufacturer's protocol as shown in table 2 and table 3. 500ng of total RNA was used per sample per reverse-transcription reaction to synthesise 500ng of cDNA. Synthesised cDNA was diluted 1:10 to 5ng/µL and a final volume of 100µL via adding 90µL of RNase free water (*Machery-Nagel*®).

Table 2. Reverse-transcription PCR mixture

Component	**Volume per 10µL reaction**
5x PrimeScript™ buffer	2µL
Primescript™ RT enzyme mix	0.5µL
Oligo dT Primer (50µM)	0.5µL
Random 6-mers (100µM)	0.5µL
RNase-free water	YµL (Y = 10 – (3.5 + X)
500ng of total RNA	XµL
Total volume	**10µL**

Table 3. Reverse-transcription thermal cycles

Step type	Time	Temperature (°C)
Reverse Transcription	15 minutes	37°C
Inactivation of RT	5 seconds	85°C
Holding stage	∞	4°C

2.5.3 Real-time PCR

For the preparation of the master mix for real-time PCR, 2x SYBR® Premix Ex Taq and ROX Reference Dye (*Takara*™) mix was used in conjunction with forward and reverse primers (*SIGMA*®) specific for various protein targets as listed in table 4. The thermal cycles for real-time PCR (Table 6) were conducted using the StepONE 96-well real-time PCR machine (*Applied Biosystems*®) using real-time PCR reaction mix composition described in table 5.

Table 4. List of targets and their primer sequences

target	**Primer sequence**
h18S	Forward: 5’ TAACGATGCCGACTGGCGATG 3’
	Reverse: 5’ AGACTTTGGTTTCCCGGAAGCT 3’
USP3	Forward: 5’ CCTCCTGAGTAGCTGGGATTA 3’
	Reverse: 5’ CACCCTAGCCAACATGGTAAA 3’
OTUB1	Forward: 5’ ACCTATCTACTCCTGAGCTTCC 3’
	Reverse: 5’ AAGAAGGGAAGGAAGCAGAAC 3’
UCHL1	Forward: 5’ CTGGGATTTGAGGATTCAG 3’
	Reverse: 5’ GCCTGTATGGCCTCATTCTT 3’

Table 5. real-time PCR reaction mix composition

Reagent	Volume (per well)	Volume (30 wells)
SYB R® Premix Ex Taq (2X) plus ROX	5µL	150µL
10µM Forward Primer	0.4µL	12µL
10µM Reverse Primer	0.4µL	12µL
RNase free dH_2O	2.2µL	66µL
cDNA template (10 ng)	2µL	60µL
Total Volume	**10µL**	**300µL**

Table 6. qPCR thermal cycle sequences

Cycles	Time	Temperature	Step type
1	2 minutes	95°C	Polymerase activation
1	5 seconds	95°C	Denaturing
40	15 seconds	60°C	Annealing/Extension

2.5.4 mRNA quantification

Relative quantification was determined based on the reference, an endogenous standard gene, (ref), which was 18S. This was achieved by measuring the number of cycles necessary to produce sufficient quantities of cDNA to pass threshold. The number of cycles was recorded for each target as its C_T value. This was repeated using five samples for each target and the C_T values were averaged. These average C_T values were then compared to the reference gene to give a normalised ΔC_T value as shown in the equation below. Following this, the ΔC_T value for each target was

converted to a fold-change in expression using the second equation below to allow for the comparison of the target genes based on their calculated expression.

ΔC_T (UT) = C_T (GOI, UT) − C_T (18S, UT)

Fold expression = $2^{-\Delta C_T (UT)}$

2.6 USP3 Knockdown

In an attempt to determine the significance of USP3's expression on DEPTOR stability, we used a silencing RNA to remove USP3 in isolation to examine the effects of changing USP3 expression without any confounding effects. To achieve this, 1.1B4 cells were incubated in a mixture of 9µL lipofectamine 2000 (*Thermo Fisher Scientific*) and 30µL of USP3 siRNA (100pmol) (*Thermo Fisher Scientific*) or 30µL of scrambled siRNA (*Thermo Fisher Scientific*) to act as a control. This mixture was left on the cells for 24 hours before it was aspirated, and fresh media was added leaving the cells to grow and reach target confluence for 72 hours. Following this, the 1.1B4 cells were extracted and analysed using the methods previously described in **2.2.3, 2.3.1, 2.3.4, 2.3.5, and 2.3.6**. The only deviation from the previously described methodology was the use of DEPTOR as a target for potential change and USP3 as a control.

Results

3.1 General cell viability

Figure 6: Changes in cell viability, metabolism and autophagy in response to hyperuricemic condition.

Cells were cultured under physiological normal (300µM UA) and hyperuricemic conditions (500µM UA) for 72 hours. Following this, live cell assays were used to perform cell viability analysis normalising to untreated cells (UT).

(A) Represents total cell count and relative levels of early and late stage apoptosis in 1.1B4 cells.
(B) Represents total cell count and relative levels of early and late stage apoptosis in MIN6 cells.
(C) Represents cellular metabolism levels in 1.1B4 cells.
(D) Represents cellular metabolism levels in MIN6 cells.
(**E)** Represents cellular autophagy levels in 1.1B4 cells.
(F) Represents cellular autophagy levels in MIN6 cells.
Data is represented as mean ± SEM.
p-values vs 300µM were calculated via Student t-test with a Tukey post-hoc analysis, p-values vs untreated cells were calculated using a one-way ANOVA with a Tukey post-hoc analysis.
* = $p < 0.05$ vs 300µM UA, # = $p < 0.05$ vs untreated cells (UT), n.**s.** = $p > 0.05$, n = 5.

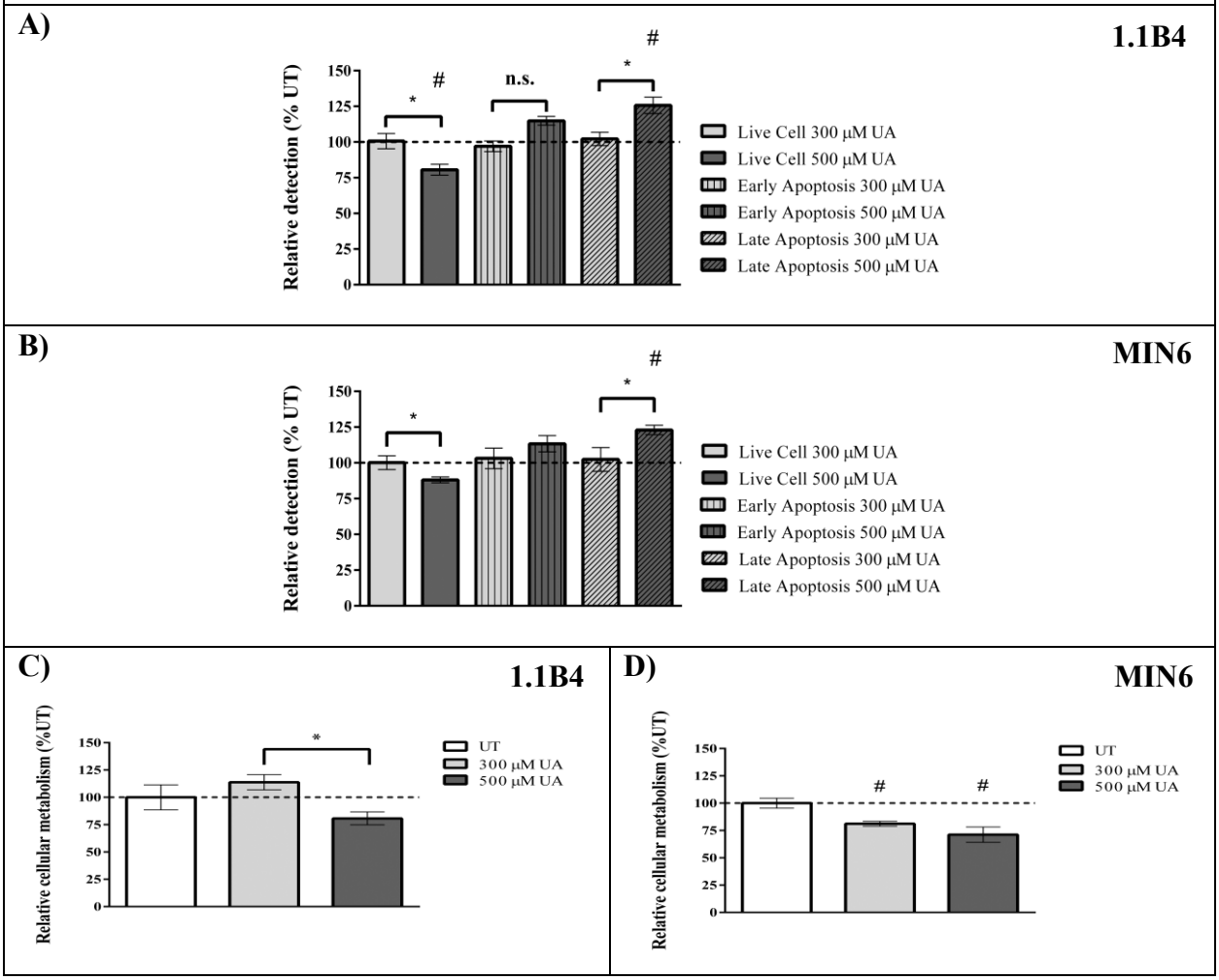

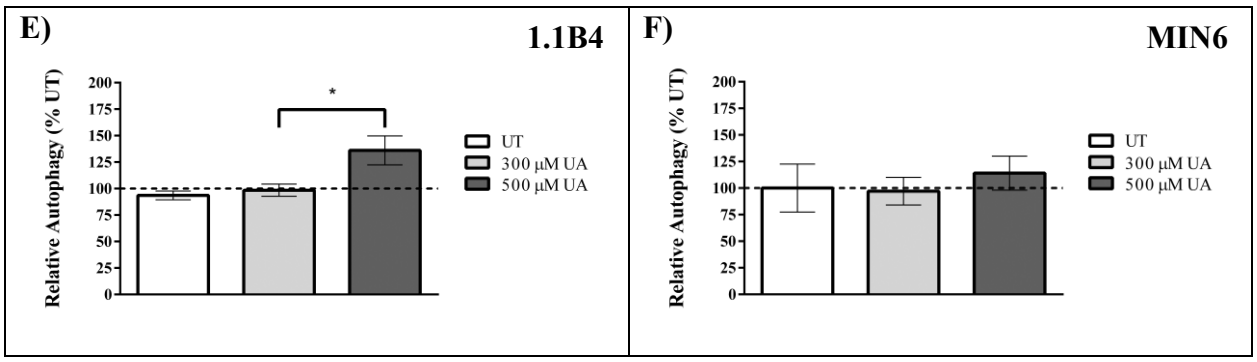

To initially establish, if changes in DEPTOR ubiquitination that may arise due to hyperuricemic conditions result in measurable changes in cell functionality and viability, we chose to measure multiple factors that are both critical to healthy cell function and are regulated by changes in DEPTOR expression. To measure changes in cellular metabolism, cellular apoptosis and autophagy, cells were treated with 300µM uric acid representing normal conditions, 500µM uric acid representing hyperuricemic condition, and PBS vehicle treated cells representing an untreated control over 72 hours. Following this, live cell assays were performed as outlined above in sections **2.3**, **2.4**, and **2.5**, respectively.

3.1.1 Cellular Apoptosis

The cell viability measure was determined by the effects of hyperuricemia on live cell count and the prevalence markers indicative of early and late stages of apoptosis. The live cell count of 1.1B4 cells resulted in a statistically significant decrease down to 80% ± 6 when compared to the cells treated with human physiological normal conditions (Fig. 6A). In the mouse (MIN6) cells, we observed a statistically significant decrease down to 88% ± 2 (Fig. 6B) when compared to cells treated with human physiological normal conditions. In terms of early stage apoptosis, both cell lines trend towards an increase in apoptotic cells but neither of these trends yield a statistically significant result.

Finally, the late stage apoptosis marker leads to significant increases as a result of human hyperuricemic condition in both human (1.1B4) and mouse (MIN6) cells with the human late apoptotic cell response of 125% ± 5 (Fig. 6A) of the untreated and an increase of 23% compared to the physiological normal treated cells. The MIN6 cells exhibited a significant late apoptotic marker expression of 123% ± 3 (Fig. 6B) of the untreated and an increase of 21% compared to the cells treated under human physiological normal condition.

3.1.2 Cellular Metabolism

Mitochondrial metabolism is key to maintaining cellular energy. Using an MTT assay we directly measured the rate of cellular metabolic activity. Metabolic activity was significantly decreased when cells were exposed to human hyperuricemic conditions with the human cells showing a significant decrease compared to the cells treated with human physiological normal uric acid levels of 27% ± 9 (Fig. 6C) of the untreated cells. In mouse (MIN6) cells, although there was no significant difference between the cells treated with hyperuricemic and human physiological normal levels, however, both treatment groups had significantly lower cellular metabolism than the untreated control with human physiological normal down to 81% ± 18 and hyperuricemic condition down to 71% ± 28 (Fig. 6D).

3.1.3 Cellular Autophagy

Using the previously described autophagy assay (**2.4.2**) we analysed the changes in cellular autophagy in response to hyperuricemic conditions as shown in figures 6E and 6F. We determined that in both, the human and mouse cells, there was a trend towards an increased autophagy as a result of exposure to hyperuricemic conditions, however, this trend only proves statistically significant ($p < 0.05$) in the human cell line with relative autophagy increased by 37% ± 14 of the untreated control and compared to human physiological normal (300μM) condition (Fig. 6E).

3.2 DEPTOR ubiquitination

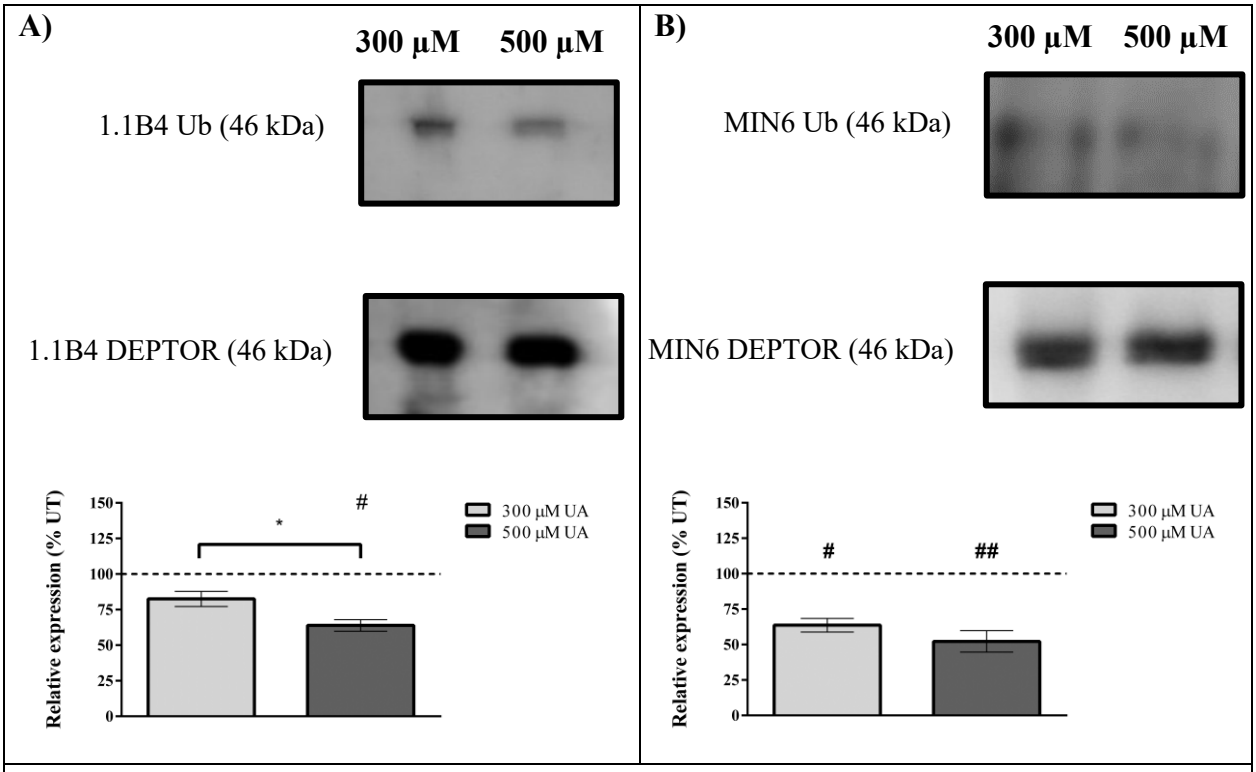

Figure 7: Changes in DEPTOR ubiquitination in response to hyperuricemic condition. 1.1B4 or MIN6 cells were cultured under physiological normal (300µM UA) and hyperuricemic conditions (500µM UA) for 72 hours. Following this, the cell lysates were used to perform a DEPTOR-based co-immunoprecipitation followed by western blot analysis with the resulting protein levels calculated by normalisation to DEPTOR and to untreated cells (UT).
(A) Represents DEPTOR ubiquitination in 1.1B4 cells.
(B) Represents DEPTOR ubiquitination in MIN6 cells.
Data is represented as mean ± SEM.
p-values vs 300µM were calculated via Student t-test with a Tukey post-hoc analysis, p-values vs untreated cells were calculated using a one-way ANOVA with a Tukey post-hoc analysis.
* = $p < 0.05$ vs 300µM UA, # = $p < 0.05$ vs untreated cells (UT), ## = $p < 0.01$ vs untreated cells (UT), n = 4.

Using co-immunoprecipitation, we isolated a set amount of DEPTOR from the total sample protein and examined the effects of hyperuricemic condition on the binding of ubiquitin as a means of detecting changes in the degradation signal that would be necessary to facilitate the changes in cell function we observed previously. Employing this isolated DEPTOR we were able to determine that both human and mouse cells have relatively lower levels of bound ubiquitin as a result of exposure to human hyperuricemic condition. In the 1.1B4 cells we were able to observe a significant

decrease in ubiquitination in the cells treated under human hyperuricemic conditions when compared to the untreated and physiological normal condition resulting in a drop down to 64% ± 4 (Fig. 7A) of the untreated control.

In MIN6 cells, although the trend towards a difference between the ubiquitination of the cells treated under human physiological and hyperuricemic condition did not prove to be statistically significant. However, we did observe that both treatments exhibited a significant decrease compared to the untreated control with human physiological condition resulting in 37% ± 4 (Fig. 7B) change, and with the cells exposed to hyperuricemic condition dropping down to 52% ± 7 as illustrated in figure 7B.

3.3 Expression of DEPTOR ubiquitination regulating proteins

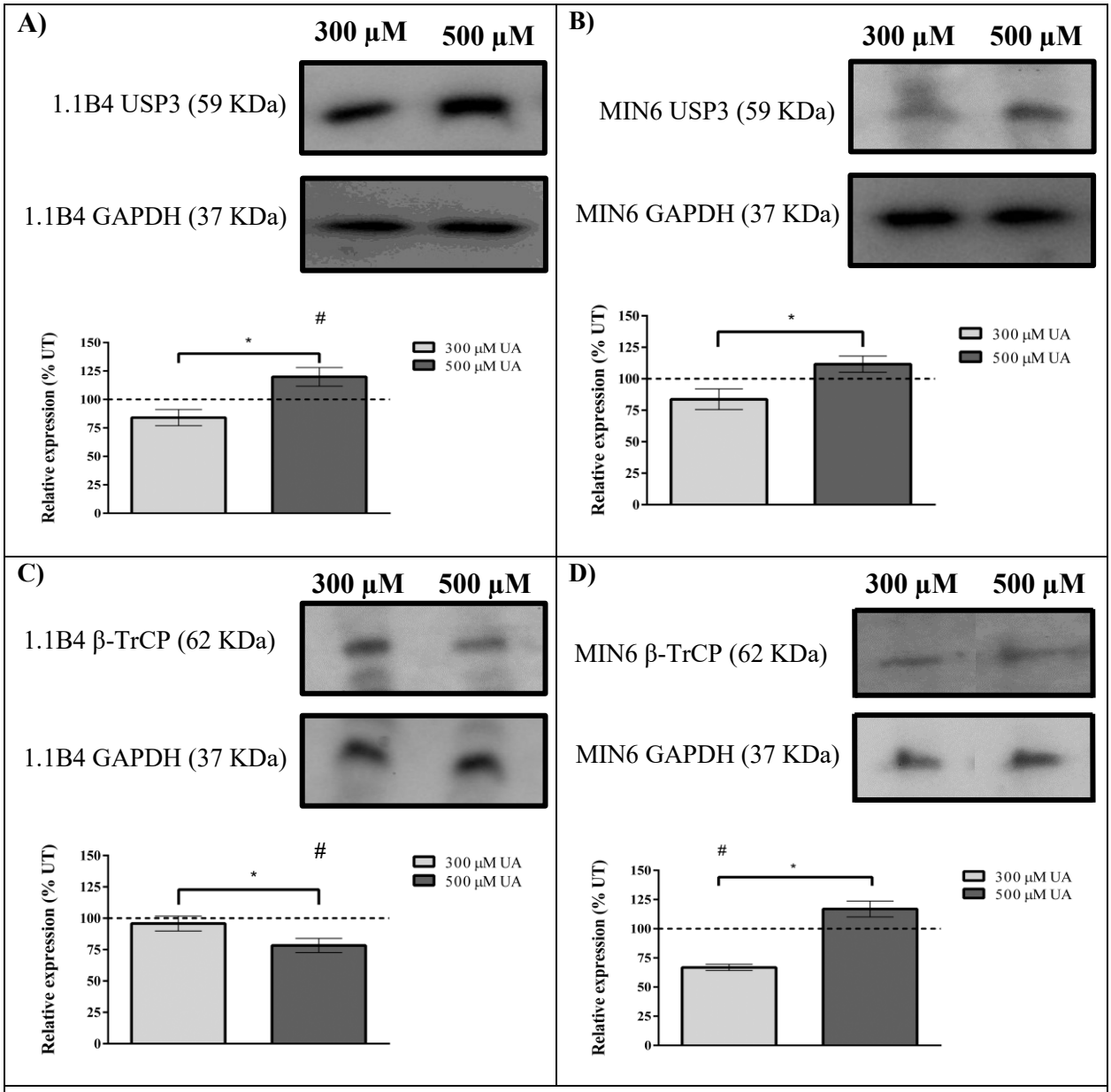

Figure 8: Changes in regulation of DEPTOR ubiquitination in response to hyperuricemic condition.

1.1B4 or MIN6 cells were cultured under human physiological normal (300µM UA) and hyperuricemic conditions (500µM UA) for 72 hours. Following this, cell lysates were used to perform a western blot analysis with the resulting protein level calculated by normalisation to GAPDH as a loading control and then to the untreated cells (UT).

(A) Represents USP3 expression in 1.1B4 cells.
(B) Represents USP3 expression in MIN6 cells.
(C) Represents β-TrCP expression in 1.1B4 cells.
(D) Represents β-TrCP expression in MIN6 cells.

Data is represented as mean ± SEM.

p-values vs 300µM were calculated via Student t-test with a Tukey post-hoc analysis, p-values vs untreated cells were calculated using a one-way ANOVA with a Tukey post-hoc analysis.

* = $p < 0.05$ vs 300µM UA, # = $p < 0.05$ vs untreated cells (UT), n = 5.

Once we had confirmed the change in ubiquitination of DEPTOR the next step was to analyse how proteins that are known to play a role in DEPTOR ubiquitination are a potential target for the removal of ubiquitin in response to hyperuricemic conditions. Also, we wanted to determine, if this change is sufficient to explain the changes we see in DEPTOR regulation. Applying western blot analysis, we determined that both human (1.1B4) and mouse (MIN6) cells see significant increases in ubiquitin specific protease 3 (USP3) expression as a result of hyperuricemic condition when compared to the levels of expression we see under human physiological normal conditions. Human cells exhibit a 35% ± 8 (Fig. 8A) increase compared to the cells treated at physiological normal. Additionally, this result is significantly greater than the untreated control cells being equal to 119% ± 8 of USP3 expression under untreated condition. In MIN6 cells, we detected a less dramatic shift with USP3 expression trending towards an increase compared to the untreated control, however, this fails to reach statistical significance with the only significant difference being between the cells treated under human physiological conditions and those treated to hyperuricemic conditions which saw a comparative increase in expression equal to 27% ± 6 (Fig. 8B).

Working in opposition to the deubiquitinating effect of USP3 is the E3 ligase β-TrCP. As with USP3, we investigated β-TrCP to see if the effect on ubiquitination was purely due to increased ubiquitin turn-over or if a reduction in initial ubiquitination was the culprit or if it was a combination of the two. Following this examination, we found that human and mouse cells appear to have differing β-TrCP responses to changing uric acid exposure. In the case of the human cells, β-TrCP expression significantly decreased down to 78% ± 13 (Fig. 8C) of the untreated cells when treated under human hyperuricemic condition, a level of 17% ± 8 lower than those treated under human physiological normal condition. This trend in β-TrCP was reversed in mouse cells, were we see a drop in β-TrCP expression in cells under human physiological conditions down to 60% ± 6

of the expression presented in the untreated cells with the cells treated under human hyperuricemic condition reaching expression levels of 50% ± 6 greater than those of the human physiological normal treatment group (Fig. 8D).

3.4 Uric acid binding to DEPTOR

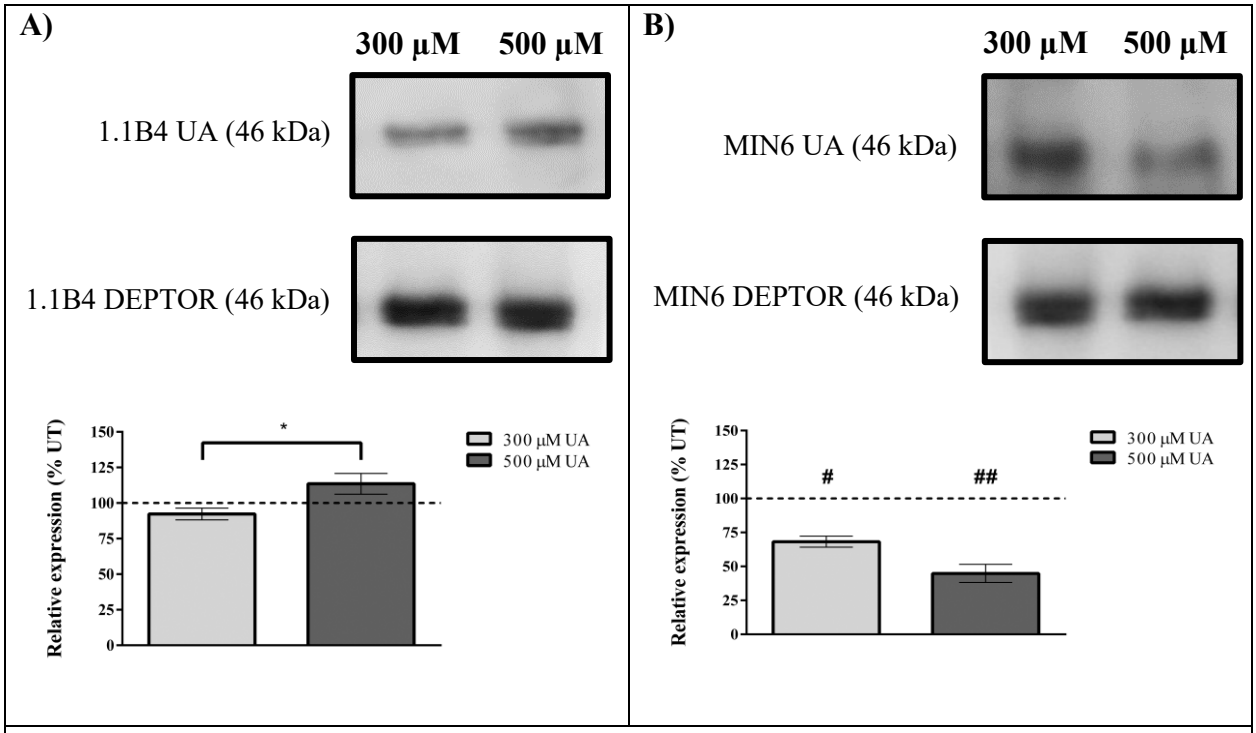

Figure 9: Detection of DEPTOR-bound uric acid in response to hyperuricemic condition.
1.1B4 or MIN6 cells were cultured under human physiological normal (300µM UA) and hyperuricemic conditions (500µM UA) for 72 hours. Following this, cell lysates were used to perform a DEPTOR-based co-immunoprecipitation followed by western blot analysis with the resulting protein level calculated by normalising to DEPTOR and to untreated cells (UT).
(A) Represents DEPTOR-bound uric acid in 1.1B4 cells.
(B) Represents DEPTOR-bound uric acid in MIN6 cells.
Data is represented as mean ± SEM.
p-values vs 300µM were calculated via Student t-test with a Tukey post-hoc analysis, p-values vs untreated cells were calculated using a one-way ANOVA with a Tukey post-hoc analysis.
* = $p < 0.05$ vs 300µM UA, # = $p < 0.05$ vs untreated cells (UT), ## = $p < 0.01$ vs untreated cells, n = 4.

Following the detection of USP3 and β-TrCP, the next question was, what is triggering these changes in DEPTOR ubiquitination and if it can't be explained through changes in protein levels. To this end, we also exposed DEPTOR isolated through co-immunoprecipitation to a uric acid-

detecting antibody to investigate the possibility that uric acid may be directly binding to DEPTOR resulting in changes in the ubiquitination dynamic. We found that not only did we detect uric acid bound to DEPTOR indicating that it was acting in a manner similar to a posttranslational modification but that it also changed with changes in uric acid concentration. In MIN6 cells, this change is actual inverse to the uric acid concentration as shown in figure 9B. We revealed that not only is there a significant decrease in the detection of uric acid bound to DEPTOR when compared to the untreated control cells of down to 68% ± 4 (300μM UA) and 44% ± 6 (500μM UA), respectively, but also a significant difference when you compare mouse cells subjected to human physiological normal level. Hyperuricemic treatment of 1.1B4 cells resulted in an increase of uric acid-bound by 23% ± 7 (Fig. 9A) compared to untreated cells.

In addition, human cells show a significant increase in bound uric acid under hyperuricemic conditions when compared to the cells under human physiological normal condition by 21% ± 8 (Fig. 9A) of the binding found in the untreated group. It should be noted that these differences were not significantly different when compared to the untreated control group.

3.5 Analysis of deubiquitinase expression in the 1.1B4 cells

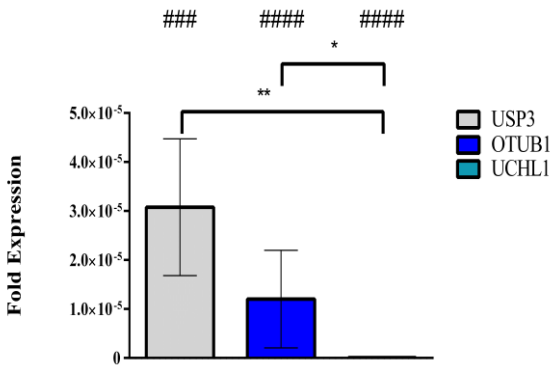

Figure 10: Analysis of deubiquitinase synthesis in 1.1B4 cells.
Total RNA of 1.1B4 cells was extracted and used in qPCR experiments to determine the relative expression of USP3 compared to ovarian tumour domain-containing ubiquitin aldehyde-binding protein 1 (OTUB1) and ubiquitin carboxyl-terminal hydrolase isozyme L1 (UCHL1); C_t values were normalised to a housekeeping RNA to provide a baseline synthesis level. C_t Values were converted to fold expression data for the purpose of both comparison and display.
Data is represented as mean ± SEM.
p-values vs USP3 expression were calculated via Student t-test with a Tukey post-hoc analysis, p-values vs control RNA were calculated using a one-way ANOVA with a Tukey post-hoc analysis.
* = $p < 0.05$, ** = $p < 0.005$, ### = $p < 0.0005$ vs control RNA, #### = $p < 0.0001$ vs control RNA, $n = 4$.

As a result of the time spent on this project new work had been published that may help to shed light on the nature of the mechanism we are trying to decipher. To this end, in an attempt to better understand the implications of recently published work investigating potential DEPTOR deubiquitinases, we have compared USP3 expression to deubiquitinases proposed in Zhao *et al.*, 2018 which were shown to have an effect on DEPTOR ubiquitination under a differing stimulus. We found that the primary deubiquitinase (OTUB1) proposed by Zhao *et al.*, 2018 has a slightly lower but not significantly different expression when compared to USP3, however, another candidate that was also put forward as a one likely to be of key importance for DEPTOR regulation (UCHL1) was found to be significantly lower expressed when compared to both USP3 and OTUB1 (Fig. 10).

3.6 USP3 knockdown

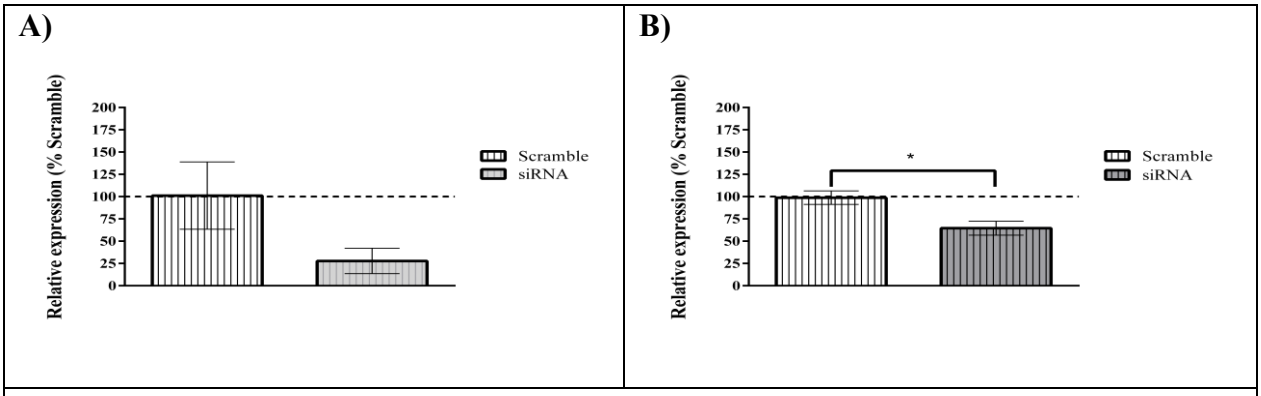

Figure 11: USP3 knockdown.
1.1B4 cells were treated with a USP3 siRNA to investigate the effects of isolated decreases in USP3 on DEPTOR expression. These cells were compared against cells treated with a random siRNA scramble which was used as a baseline control against the USP3 siRNA and as a control for the transfection process.
(A) Represents USP3 expression measured by western blot
(B) Represents DEPTOR protein levels
Data is represented as mean ± SEM.
p-values vs siRNA scramble were calculated via Student t-test with a Tukey post-hoc analysis.
* = $p < 0.05$ vs siRNA scramble, DEPTOR: n = 4, USP3: n = 2.

As a result of the effects observed on USP3 expression due to uric acid treatment and with the new insight provided by new research being published, we chose to investigate the significance of decreased USP3 expression in isolation to any other factor that may arise as a result of treatment with uric acid. To this end, we were able to run initial tests on 1.1B4 cells and although we did not generate sufficient data to allow for statistical analysis, the trends displayed in Figure 11A indicates that USP3 knock-down seemed to have been successful. In the case of DEPTOR expression, we found that silencing of USP3 resulted in a significant reduction of DEPTOR expression by 30% ± 11 compared to scrambled control (Fig. 11B).

Discussion

4.1 Impacts on Cellular viability and function

Diabetes mellitus (DM) comes with specific changes in pancreatic β-cell function that denote the initiation or progression of T1DM or T2DM. In the case of T1DM, the initial loss of pancreatic β-cell mass starts further irreversible loss of pancreatic function as β-cell mass continues to decrease in response to increased stress due to the remaining cells trying to compensate for the loss of insulin secretion (Jaberi-Douraki *et al.*, 2015). In T2DM, the initial stages, although caused by the development of peripheral resistance to insulin signalling, leading to the loss of β-cell mass as a result of the stress caused by over-signalling as a compensatory mechanism to overcome the lack of insulin sensitivity (Rojas *et al.*, 2018). Hence, the irreversible disease progression leads to far greater rates of T2DM-related complications, once patients have passed a critical point of β-cell mass loss (Munnee *et al.*, 2016). These observations put the loss of β-cell mass into the spotlight independent of the type of DM. Thus, deciphering the molecular mechanisms of pancreatic β-cell mass loss is paramount.

This study investigated the molecular mechanisms of pancreatic β-cell death based on hyperuricemic conditions, as high plasma uric acid levels been correlated with DM (Krishnan *et al.*, 2013). Firstly, we determined that elevated extracellular uric acid levels resembling high serum uric acid caused significant changes in the viability and metabolic rate in both the human (1.1B4) and mouse (MIN6) pancreatic β-cells. These changes include a decrease in cellular metabolism (Fig. 6C, Fig. 6D), and live cells (Fig. 6A, Fig. 6B) which was matched with significant increases in apoptosis in both cell lines and autophagy in human cells (Fig. 6D). These changes indicated that hyperuricemic condition can create effects similar to that seen in T1DM development and T2DM progression. This first set of evidence is in line with existing data showing that patients with T2DM exhibit elevated levels of autophagy gene expression (Masini *et al.*, 2009) caused by an inhibition of the main autophagy regulator, mTORC1. Furthermore, an increase in autophagy due

to changes in mTORC1 activity was demonstrated to have negative impacts on diabetics (Zoncu *et al.*, 2011) with the damaging effects increasing over time (Bartolome & Guillén, 2014).

These observations lead to the question of how the changes in mTORC1 activity arises and if they can be prevented to halt the devastating progress of β-cell mass loss. Interestingly, based on further evidence discussed in the following chapters we can likely link apoptotic events to the observed decrease in cellular metabolism as it is likely to be the initial step in the cellular response that results in the observed increase in apoptosis and reduction in total live cells. This idea is supported by the fact that starvation is known to cause this exact effect as a means of reducing the bodies' energy demand through the reduction of total cell mass (He & Klionsky, 2009. Munson & Ganley, 2015). However, this is not the full story as cells have multiple ways of adjusting themselves to reduced cellular metabolism before an apoptotic response is triggered. One such counter to loss of energy production is increasing autophagic signalling as a means of reducing cellular energy demand and recovering energy from unneeded proteins and organelles (He & Klionsky, 2009). This idea is supported by our data which shows autophagy increases significantly in 1.1B4 cells in response to hyperuricemic condition indicating that in addition to driving down metabolic activity hyperuricemic condition is also enough to trigger an increase in autophagy (Sheng *et al.*, 2017). These two factors explain why we see an increase in apoptosis markers and a decrease in live cell counts as the reduced metabolic activity would reduce the rate of cell growth and the increased autophagy would trigger increased cell death. These effects would likely be sufficient to cause the development of DM in patients as this loss of cell mass has been linked with the formation and progression of DM (Pipeleers *et al.*, 2008), and even in the cases that did not result in total β-cell mass loss pharmacological inhibition of the mTOR complexes has been shown to cause diabetes like hyperglycaemia and insulin resistance in patients (Vergès & Cariou, 2015). However, this fails to provide an effective target for the treatment of DM as these studies fail to provide a mechanism

by which hyperuricemic condition triggers these changes. To base a treatment on the fact that simply modulating the mTOR complexes will solve the problem without understanding this mechanism may have severe off target effects such as tumorigenesis as other cells are pushed into an abnormal growth state. A possible target to treat DM could be DEPTOR, the negative regulator of mTOR complexes (Catena & Fanciulli, 2017).

4.2 Changes in DEPTOR regulation due to hyperuricemia

Focusing on the fact that we detected a change in metabolic activity and autophagy in a nutrient-independent fashion we decided to investigate if DEPTOR expression was changed in response to hyperuricemic conditions. It is well documented that DEPTOR is capable of modifying metabolic activity and autophagy within cells through its regulatory effects on the mTOR complexes (Catena & Fanciulli, 2017). The current literature focuses mostly on DEPTOR and its role in the development of cancer (Li *et al.*, 2014) as a loss of DEPTOR function increases cell growth by shifting the cellular metabolism to a high energy state (Caron *et al.*, 2017). Our previous work on human pancreatic β-cells (1.1B4 cells) revealed DEPTOR protein levels are increased under hyperuricemic conditions, which made it a prime candidate for the regulator of the changes we observe in cell viability. In addition, we could prove that the increase in DEPTOR protein level is not based on an increase in transcriptional activity (Cain, 2017). An increase in DEPTOR protein could also be explained by stabilising DEPTOR protein due to a change in its ubiquitination. This would be in line with other disease models in which DEPTOR's stability is increased by reducing its ubiquitination (Wang *et al.*, 2012). Examples include ankylosing spondylitis in which increased DEPTOR stability resulted in increased autophagy (Zhai *et al.*, 2018), and in pituitary adenoma where increased DEPTOR stability increased autophagy and cell death (Yao *et al.*, 2019). We can confirm the amount of ubiquitin bound to DEPTOR decreased significantly in mouse and human

pancreatic β-cells. In the human β-cells, we found a significant decrease in the cells exposed to hyperuricemic condition when compared to both the, untreated and physiological normal cells (Fig. 7A). In the mouse cells, we do see significant decreases when compared to the untreated cells but between the human physiological normal and hyperuricemic treatment conditions we didn't find the trend towards decrease to be significant, however, this is likely again due to the high uric acid concentrations we applied to the MIN6 cells (Fig. 7B).

This decrease in DEPTOR ubiquitination would create effects in line with the existing literature where studies have shown that increased DEPTOR activity leads to decreased cellular proliferation, cellular metabolism and cellular growth (Catena & Fanciulli, 2017. Li *et al.*, 2014. Zhao *et al.*, 2005). In this study, we observe the trend of DEPTOR expression resulting in an inverse effect on cellular viability. Targeting DEPTOR expression as a means of treatment for DM is both easier and less likely to have off target effects as would be the case in trying to target general changes in cell metabolic activity or autophagy. This presents us with another question, that being what is responsible for the changes we observed in DEPTOR ubiquitination, and can these changes be reversed or modulated to act as a treatment for disturbed cell growth and viability. Although this does provide an answer to how the changes in cell viability and function occur, it also raises the question of how this change in ubiquitination is being achieved as this may provide a more specific treatment target or illuminate an unknown mechanism for DEPTOR protein ubiquitination.

4.3 Expression of ubiquitination regulating proteins

Firstly, we investigated the known ubiquitin E3-ligase of DEPTOR, β-TrCP (Wang *et al.*, 2012), where its disturbance is known to result in pathologic changes in cellular function (Zhao & Sun, 2012). β-TrCP protein level is significantly reduced under hyperuricemic conditions in human β-cells (Fig. 8C) and also in mouse cells when compared to the untreated control (Fig. 8D). The

consequence of this down-regulation of β-TrCP under hyperuricemic conditions ultimately is less ubiquitination and higher DEPTOR protein stability. The impacts of this higher DEPTOR stability is an increase of mTOR complex inhibition and a reduction of cell growth and viability as well as cellular metabolism. This matches with the outcomes we would come to expect based on the previously discussed understanding of the consequences of changes to DEPTOR stability, however, this is the first study to examine the effect of uric acid on β-TrCP expression so there is no data with which to compare.

In addition to the pro-ubiquitination signal generated by the E3 ligase β-TrCP, it has recently been shown that there are also proteins responsible for the deubiquitinating of proteins, called DUBs or ubiquitin specific proteases (USPs, Heideker & Wertz, 2015). This raises the need for further examination as this process may also be disturbed by hyperuricemic conditions which would further alter DEPTOR ubiquitination beyond changes in β-TrCP. If DUBs or USPs are changing under hyperuricemic conditions, it would limit the effectiveness of targeting β-TrCP as a treatment option for returning DEPTOR ubiquitination back to normal levels. As these deubiquitinating proteins are only a recent addition to our understanding of the protein ubiquitination dynamic, they are not yet well categorised or characterised (Farshi *et al.*, 2015). At the start of this project, DUBs or USPs controlling DEPTOR deubiquitination were unknown. Analysis revealed USP3 as a potential target as it was known to be highly expressed within the pancreas (Sloper-mould *et al.*, 1999) and has been shown to interact with other cell proliferation targets (Fu *et al.*, 2017). We did find a significant increase in the protein level of USP3 under hyperuricemic conditions in both human and mouse pancreatic β-cells strongly indicating that exposure to high concentrations of uric acid has shifted protein level to favour DEPTOR's deubiquitination over is ubiquitination. This points to USP3 being key to changes we see in overall cell function and provides a potential target as a means of alleviating uric acids role in DM progression. This would also provide the first

evidence that both USP3 and potentially deubiquitinating enzymes as a whole may be regulated by uric acid (Fig. 8A). Although this would be the first evidence linking USP3 to uric acid the changes we have observed are similar to what we would expect based on the existing research has linked the general function of DUBs and USPs to the regulation of cellular pathways responsible for cellular growth, proliferation, turn over and apoptosis (Daviet & Colland, 2008). With respect to USP3 specifically the current literature links its expression to cellular proliferation and survivability through altering the stability of targets including p53 and histones (Fu *et al.*, 2017). Also, studies where inhibitors have been applied to decrease USP3 function, have been shown to lead to runaway cell proliferation (Fu *et al.*, 2017). The observed change in USP3 expression is in line with our expectation of changes in DEPTOR ubiquitination, however, it is unknown if USP3 does in fact interact with DEPTOR.

4.5 Examination of USP3 expression in the pancreas

With previous experiments indicating that USP3 may play a major role in DEPTOR ubiquitination it becomes important to find ways to confirm interactions between these two proteins. To confirm its importance, we compared USP3 expression to OTUB1 and UCHL1. This choice was based on the only study on potential DEPTOR deubiquitinases which put both, OTUB1 and UCHL1, forward as key regulators of DEPTOR ubiquitination (Zhao *et al.*, 2018). Zhao and co-workers measured different deubiquitinases as candidates for DEPTOR deubiquitination in order to elucidate the mechanism underlying an observed change in DEPTOR protein level in response to amino acid level changes. This study examined a key factor that was mirrored by our own investigation, demonstrating ubiquitination may be regulated by extracellular nutritional factors. Increasing amino acids in the culture media replicates a process which in humans can only occur as a result of increased uptake from dietary sources in the same way that uric acid is increased by

diet. Since both experiments evaluate a similar physiological trigger being extracellular nutrient level, it is not unreasonable to compare the mRNA expression of the published DUBs with the expression of USP3 in 1.1B4 cells as a means of evaluating the potential relevance of USP3's effect on DEPTOR. This experiment revealed that not only is the expression of USP3 equal to that of OTUB1 which was selected as the most important regulator of DEPTOR ubiquitination. USP3 was significantly more expressed than UCHL1 which was identified as another significant regulator of DEPTOR (Zhao *et al.*, 2018). These results by Zhao and co-workers can be explained by additional findings exhibiting that numerous deubiquitinases are capable of interacting with DEPTOR. It suggests that deubiquitinases have multiple targets, and that their effect is likely controlled through limiting their expression levels either through the effects of direct stimuli such as changes in uric acid, or amino acid concentrations, or due to different expression profiles in different tissue types such as the differing distribution we see with USP3 (Heideker & Wertz, 2015. Sloper-mould *et al.*, 1999). This would be supported by our investigation into USP3 expression within the pancreas as it showed levels equal to or significantly greater (Fig. 10) than some of the targets put forward in Zhao's study.

To further prove the significance of UPS3 we performed a targeted inhibition of USP3 through the use of a silencing RNA. Although we were unable to confirm the significance of the trend towards USP3 silencing (Fig. 11A), the strength of the trend and the resulting change in DEPTOR expression (Fig. 11B) makes a strong argument for its success. As a result of this experiment, we were able to show that the specific inhibition of endogenous USP3 in 1.1B4 significantly reduced the expression of DEPTOR. This result in combination with the previous evidence of USP3 regulation by hyperuricemic conditions provides a strong case that we have identified USP3 as a new and major regulator of DEPTOR expression. When combined with the β-TrCP expression data these observations provide the first evidence for uric acid directly regulating protein ubiquitination

and more specifically DEPTOR ubiquitination. In addition, because USP3 has been linked to the regulation of DNA damage (Lancini *et al.*, 2014) this may also explain why we see certain cells having strenuous damage responses in low uric acid conditions as a result of USP3 inactivity creating a reduction in DNA damage detection.

With this new understanding of the effects of USP3 and β-TrCP on DEPTOR, it raises the question of if the changes in β-TrCP/USP3 are the only effects mediated by elevated uric acid levels.

4.6 Uric acid as a ubiquitination modifier

With the results of previous experiments showing that hyperuricemic conditions are capable of modifying DEPTOR ubiquitination the question arises if this effect can be further elevated by direct effects of uric acid on proteins called urate-protein adducts or uratylation (Turner *et al.*, 2018). Under normal conditions ubiquitination is regulated by the interaction between proteins and ubiquitination or deubiquitination proteins resulting in the formation of specific ubiquitin chains (Neutzner & Neutzner, 2012). We propose that uratylation disturbs this process. Uratylation as our experiment and the work of Turner and co-workers suggest is acting to interrupt the traditional ubiquitination process through the binding of uric acid or a modified version of it to a target protein in place of ubiquitin or binds to the existing ubiquitin chain modifying the length or shape thus modifying the interactions with proteins. The most likely region for this modification is a lysine residue, which is based on the fact that the vast majority of ubiquitin binding sites are lysine residues (Neutzner & Neutzner, 2012). Thus, it is only logical that the modifications that arise as a result of uric acid will share the same binding site and this has been shown in the work of Turner and co-workers, however, this does not exclude the potential for other binding sites. In the case of DEPTOR, normal ubiquitination takes the form of β-TrCP polyubiquitinating DEPTOR leading to its degradation (Zhao & Sun, 2012), provided that the ubiquitin chain is not removed by a

deubiquitinase, especially USP3. With this in mind, we chose to take the most direct route and examined DEPTOR for any potential direct interactions with uric acid. This would show if there was any direct uric acid-binding on the DEPTOR molecule as direct binding has the potential to inhibit interactions between ubiquitin regulating proteins by occupying the binding sites necessary for recognition or interaction between β-TrCP/USP3 and DEPTOR. Alternatively, detected DEPTOR-bound uric acid could prevent the formation of the polyubiquitin chain by binding to a bound-ubiquitin prematurely terminating the ubiquitin chain. This would act in a manner similar to the existing posttranslational modification, acetylation (Ohtake *et al.*, 2015). Our experiment shows what is arguably the most interesting result being that we detected a direct binding of uric acid to proteins (Fig. 9A). This result demonstrates the first cell example of uric acid binding to protein and that this binding changes in response to changes in uric acid concentration in a way that is not proportional to the concertation of uric acid that the cells were exposed to. In human β-cells exposed to hyperuricemic conditions, uratylation is significantly higher (Fig. 9A). In mouse β-cells, this trend is reversed with the β-cells treated with the highest levels of uric acid showing the lowest levels of DEPTOR bound uric acid (Fig. 9B). Both these trends indicate that instead of any binding detected being the result of increased random binding due to increased uric acid concentrations there is evidence to suggest that there is some form of regulation to the uric acid binding or that more than one protein is involved in the binding in the case of DEPTOR. This is further supported by the study by Turner and co-workers, confirming that uric acid was binding to ubiquitin. Uric acid adducts were analysed with mass spectrometry and with the detection of uratylated albumin in human serum. This study helps to reinforce our findings that detected bound uric acid is supporting evidence of previously unobserved protein modification. While this study provides proof of concept because the experiments were performed in vitro using isolated ubiquitin and uric acid or using patient samples, it is difficult to use these results to elucidate the underlying

biological regulatory mechanism. The existence of uratylation of DEPTOR or ubiquitin *in vivo* would provide an explanation for the observed correlation between hyperuricemia and diabetes as the bound uric acid would likely inhibit DEPTOR ubiquitination resulting in the changes we have previously observed in cell metabolism and viability. Furthermore, this results in the prerequisite decrease in pancreatic β-cell mass necessary to facilitate the development of T1DM or the progression of T2DM in the same way that a build-up of cytokines within a pancreatic β-cell results in the initiation of cell mass loss to an autoimmune response in T1DM (Rojas *et al.*, 2018).

4.7 Discussing causality, Diabetes vs hyperuricemia:

As a result of the interconnected nature of the dietary conditions that drive the development of both, diabetes mellitus and hyperuricemia, questions have arisen to the nature of causality between the two conditions. Some have proposed that hyperuricemia can precede the development of diabetes mellitus and may act as a driving force towards its development (Kodama *et al.*, 2009). Others, however, have proposed the rise in serum uric acid levels is simply an early indication of the effects of a diet that will lead to the development of diabetes mellitus independent of any observed changes in serum uric acid levels (Zhang *et al.*, 2016). Due to the nature of our experiments we are unable to effectively determine the nature of this causality as our experiments are only based on increased serum uric acid in isolation to any other dietary changes. The current literature shows multiple studies revealing that serum uric acid levels can act to predict the risk of developing diabetes mellitus (Tae *et al.*, 2005; Soltani *et al.*, 2013; Zhang *et al.*, 2016; Varadaiah *et al.*, 2019). This in itself indicates that there is the potential for hyperuricemia to have a causal effect on the development of diabetes mellitus. The literature also offers potential mechanisms that may provide an explanation of this effect with several studies showing that as serum uric acid levels increase uric acid shifts from an antioxidant to a pro-oxidant leading to changes in metabolism and

to the development of insulin resistance (Adnan *et al.*, 2019). However, across the literature as a whole, there are studies that have shown results that minimise or dispute these effects as this is a controversial topic. We have chosen to look at meta-analyses of the literature which have concluded the current literature supports the idea of serum uric acid as an independent risk factor for the development of diabetes mellitus (Kodama *et al.*, 2009).

4.8 What does this mean going forward

Now that we have explored what the findings of this study mean both in relation to our chosen disease model, we would like to discuss how these potential findings may be extrapolated out to apply to our general understanding of physiological principles.

The first of these will be how this study affects the understanding of uric acid and its role within the body. The current central dogma is that uric acid functions as both an excreted waste product of purine degradation (Maiuolo *et al.*, 2016) and as an antioxidant to help overcome deficiencies due to the inability of humans to synthesise vitamin c (Sevanian *et al.*, 1985). Although this study does not provide evidence to dispute these ideas, it does further support the idea that uric acid may play a larger role within the body particularly with regards to the regulation of protein level. This could lead to new avenues in the research of diseases that arise due to disturbances in cell growth regulation ranging from cancer to diabetes. A shift towards an increased focus on the importance of uric acid as a protein level regulator would also lead to an increase into the consideration of how uric acid levels may impact the dynamics of established protein regulator pathways which until now has seen little to no exploration. It is also worth considering that once you consider the importance uric acid may play on protein levels it raises the question as to how the behaviour of human cells may change when cultured in media with physiological normal levels of uric acid. It is not unreasonable to assume that the return of a substance that exists in concentrations equal to

300μM could significantly impact cellular function if through nothing more than altering concertation gradients. In addition to this, there has been some evidence to support that uric acid may function as a regulator of the cellular microenvironment via interacting with toll like receptors (Sato *et al.*, 2009). This has been shown in some cancer studies where uric acid can act as a damage associated molecular pattern triggering inflammatory responses and modifying oxidative responses in a way that is shown to persist in tumours and neighbouring regions even after the tumour has been excised (Bernardes *et al.*, 2015).

The second way this may shift existing understanding is that these results also point to the fact that uric acid may be acting as a negative regulator providing an opposing signal to that generated by nutrients like glucose. This would be explained by the fact that under normal dietary conditions uric acid concentrations increase in response to starvation or excessive activity (Cicerchi *et al.*, 2014). Normally, it would be reasonable to assume that because the conditions under which we see hyperuricemia are also ones in which there is low available energy that any reduction in energy consuming process is due to a reduction in an activating signal. However, in our experiments we, have shown that despite the cells retrieving adequate levels of glucose we still see an increase in energy conserving pathways in the form of autophagy and mTOR inhibition. This points to the potential that rather than being solely due to an absence of nutrients that energy conserving behaviour may be also driven in part or predominantly by a uric acid build up. This effect could be explained in two ways: firstly, as uric acid levels are not known to fluctuate as frequently as glucose it may be providing a redundancy that is adapted to respond to longer term changes in energy availability. Secondly, this mechanism acts as a buffer to glucose stimulation by providing a negative feedback "break" on changes in expression that arise due to increased energy levels. This breaking effect would limit cellular growth signals in the cases of unstained increases in glucose promoting a shift towards storage over growth until a stable nutrient source can be re-established.

The final impact of this study, I will be speculating on is one of the most interesting but also one of the hardest to predict as it provides such a wide range of possibilities, and that is the indications that uric acid is capable of direct binding to proteins. This is shown in our uric acid co-immunoprecipitations which indicated protein-bound uric acid (Fig. 9A, Fig. 9B), and is further supported by the previously referenced study by Turner and co-workers (Turner *et al.*, 2018) which confirmed uric acid binding to ubiquitin in a reaction tube. This finding and new process have massive implications for how we think about posttranslational modification, indicating that there may be an entirely new form of modification which, if true, would have an incalculable impact on existing protein signalling pathways. Although we cannot determine the exact mechanism behind how uric acid binds to proteins, we can make some inferences based on the results we observed. The key observation is that the binding site is most likely a lysine residue shared by ubiquitin (Turner *et al.*, 2018). The evidence to support this is that in humans β-cells we see a significant increase in uric acid binding followed by a trend towards decreasing levels of DEPTOR bound ubiquitin which could reasonably be assumed to be due to uric acid inhibiting ubiquitination through competitively binding to the same target substrate. This idea is supported by the fact that Turner and co-workers have shown that uric acid is capable of binding to ubiquitin which is only known to form bonds based on lysine targets. It is also reasonable to assume this binding between ubiquitin and uric acid is inhibitory to ubiquitin binding to ubiquitin in a way similar to that of existing acetylation resulting in the premature termination of a polyubiquitin chain (Ohtake *et al.*, 2015). Further support is found in the trend we see in the mouse data in which the reduction in bound ubiquitin approximately equals the reduction in bound uric acid (Fig. 7B, Fig. 9B) indicating that the uric acid detected is more likely to be bound to ubiquitin rather than DEPTOR. Alternatively, binding to the protein directly inhibits interactions between proteins and ubiquitinases in a manner similar to the interactions between phosphorylation and O-GlcNAc

modification (Leney *et al.*, 2017). This would result in the kind of uric acid binding that we see in the human β-cells in which we see ubiquitin and uric acid binding trending inversely (Fig. 7A, Fig. 9A) to each other indicating that uric acid binding is excluding ubiquitination. In addition to the impact of a new posttranslational modification, the way in which this is regulated also points to a potential new function of existing proteins or a new class of proteins that would be necessary to facilitate the binding of uric acid to its potential targets.

4.9 Potential model

As a means to visualise ideas we discussed regarding protein regulation, we have created a diagrammatic representation of what we believe to be the potential pathways that would result in the outcomes that we have observed. Firstly, figure 12 IA shows how DEPTOR is regulated under normal conditions, in which it is ubiquitinated by β-TrCP marking it for degradation. The first deviation from this is shown in figure 12 IB in which under low energy conditions DEPTOR is deubiquitinated (in this case by USP3) leading to the cleavage of the bound ubiquitin molecule and the degradation of the cleaved ubiquitin. The third case as shown in figure 12 IC is what we propose is happening within the mouse cells, in which the binding of uric acid to ubiquitin signalling the molecule for deubiquitination increasing the activity of USP3 thus preserving DEPTOR expression through increased ubiquitin degradation. Finally, as shown by a pathway in figure 12 II we see what we believe is happening in the human β-cells in which uric acid binds to the target protein in the same location as ubiquitin preventing the initial ubiquitination thus preserving DEPTOR expression by preventing it from being signalled for degradation.

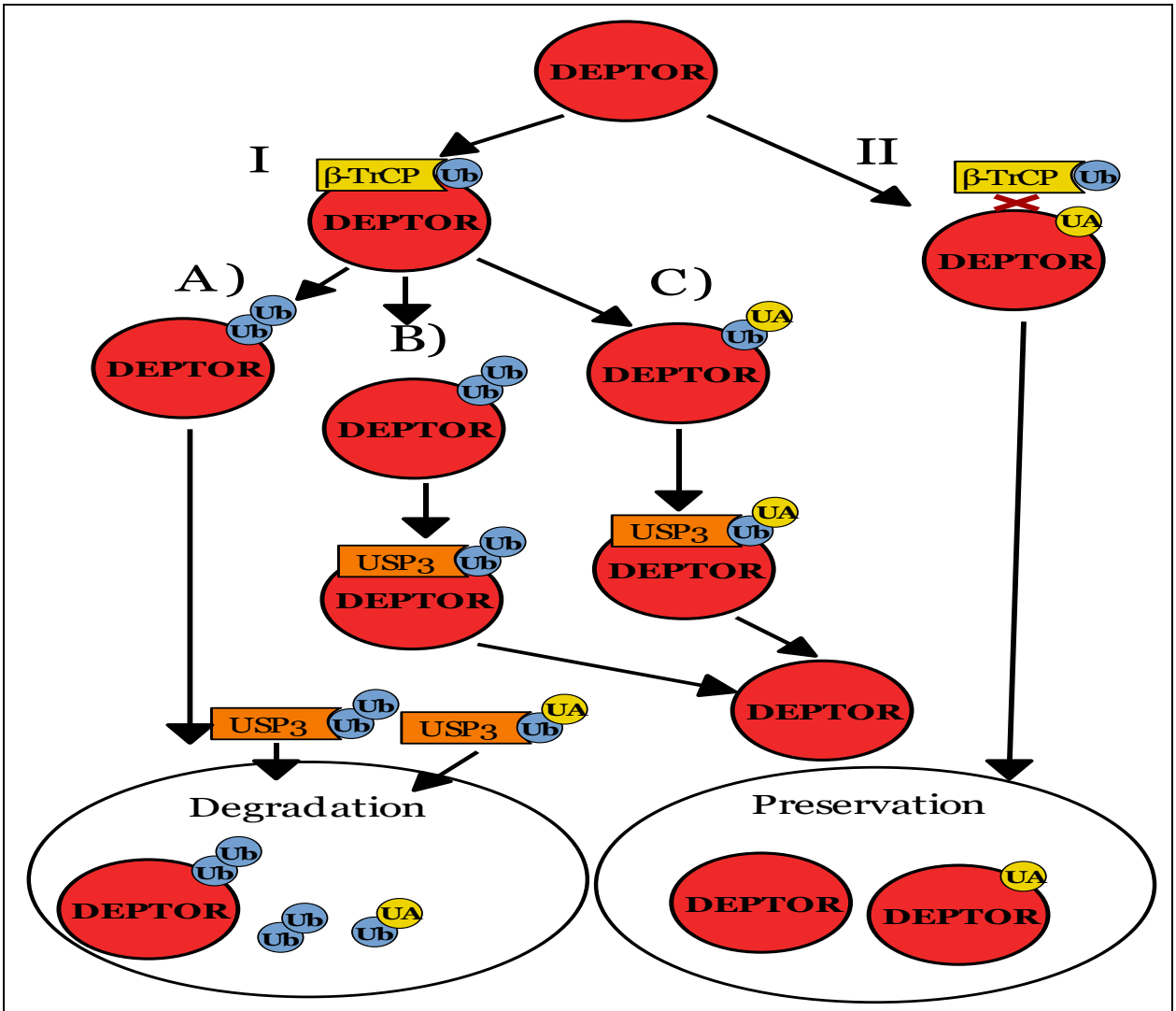

Figure 12. Potential pathways for DEPTOR ubiquitination.
This figure shows the proposed models of DEPTOR ubiquitination under the influence of differing uric acid concentrations.
(IA) represents DEPTOR ubiquitination leading to degradation.
(IB) represents the rescue of DEPTOR from its ubiquitination via the activity of the deubiquitinase USP3.
(IC) represents a potential increase in DEPTOR deubiquitination as a result of uric acid binding signalling increased activity of USP3.
(II) represents the inhibition of ubiquitination through the direct binding of uric acid to DEPTOR.

4.10 Evaluating potential animal model

For this study we chose to use two different cell lines to represent two different species, the reason for this is twofold. Firstly, by using multiple cell lines of different species it allows us to evaluate the significance of our target effects by allowing us to observe the potential for evolutionary

conservation. This provides an indication of how critical the process is for overall cell function. Secondly, it allows us to set the groundwork for an animal model to expand from cell culture experiments to whole animal studies. The advantage of whole animal experiments is that it models the consequences of interorgan signalling and multiple pathway effects that only arise as a result of the interactions between different cell types. With this in mind, it is important to evaluate how the results we see in mouse cells and human cells differ, so that we can forecast how these differences may scale out to whole animal models and how these effects may translate to the human. Our results indicate that overall cell viability and function of the cells were similar overall in both, humans and mice. The points on which the cells differ can broadly be broken down into two categories.

The first of these is the masking of trends in response to the hyperuricemic condition. This is best seen in the MIN6 cell ubiquitination data where although the human physiological normal and human hyperuricemic condition both show a significant decrease DEPTOR-bound ubiquitin. But, this is only in comparison to the untreated cells, with the resulting change being so large as to mask a smaller change that may be present between the human physiological normal and the human hyperuricemic treatment groups. This is likely because the exact cellular distribution of uricase in the mouse is unknown and the best model rat data does not include the pancreas within its testing (Motojima & Goto, 1990). As we are unable to determine if this enzyme is breaking down uric acid within the mouse cells potentially blunting the response to uric acid. This would reduce the difference between treatment groups leading to the need for a greater sample size to determine statistical significance. In addition to the potential blunting of the uric acid response, it could be possible that the difference between the mouse physiological normal serum uric acid and human physiological normal serum uric acid levels may be too great. This could lead to a diminishing returns in change to cell viability when compared to hyperuricemic conditions (estimated mouse

serum uric acid equals 75nmol/mL (de Azevedo *et al.*, 2017)) as simple treating the mouse cells with human physiological normal uric acid may trigger a hyperuricemic response within the mouse pancreatic β-cells and it is unknown if the effects of hyperuricemia have a linear, exponential, or sigmoidal relation to uric acid concentration.

The second major difference between human and mouse cells indicated by our experiments is the difference in the mechanism that underpins the changes in ubiquitination. Although we see significant changes in USP3 and β-TrCP, the impact of these changes is less clear as unlike the human the expression of both proteins seems to follow the same trend of decreasing under human physiological normal conditions but increasing under hyperuricemic conditions. This runs counter to the bound ubiquitin which is significantly decreased in both treatment groups, and which indicates that in the mouse cells the major diver for ubiquitination is not the expression of ubiquitin regulating proteins like in the human cells. As discussed previously in **4.3** and **4.4** we postulate that this process is instead regulated by the interactions between uric acid and ubiquitin. It shows why it is important to take direct measurements in protein pathway analysis. As this study shows that although the live cell assay indicates a similar phenotypical response to the hyperuricemic condition the measured protein modification levels indicate a differing mechanism which, if not accounted for, could lead to unexpected differences in response to targeted treatments. This difference in uric acid response could also explain some of the unexpected failures of certain treatments to translate from cell culture trails and or animal models into the clinic as uric acid is rarely considered in animal trials and not typically added or controlled for in cell culture media.

With these differences in mind, we can evaluate the effectiveness of the mouse as a model for human hyperuricemia. In the case of the blunted response we see, this can be accounted for by reducing uric concentrations and treating with a uricase inhibitor. This would bring uric acid back towards a level more comparable to those in the humans and the treatment with uricase inhibitors

preventing the breakdown of uric acid allowing it to build up in a manner similar to those found in the human. However, as we have put forward the likely differing mechanism responsible for the changes we have seen, this will likely limit the potential conclusion we can draw from these experiments. Overall it would best be summed up that the mouse provides a potential model for the general changes we see under hyperuricemic condition but is unlikely to provide more in-depth understanding without significant modification in the form of pharmaceutical or biological interventions.

4.10.1 The impact of nutrition

As the cell lines used are representative models for two different species it is important to also consider how this may affect the results we have achieved. One major difference between the two cell lines is how the conditions necessary to induce the disease state differ from those that the cell would usually encounter. As both diabetes mellitus and hyperuricemia are primarily driven by overnutrition derived from a diet high in fats, sugars and purines it is necessary to evaluate how this differs from the standard diet of both models and how these standards differ between models. In the case of the human, this is simple as although the type of diet necessary to initiate disease pathogenesis is not normal, it can easily be achieved through overconsumption of normal western diet (Maiuolo *et al.*, 2016). For the mouse model, however, this diet is quite different from that of a normal mouse. The evidence for this is the straight forward lack of diabetic or hyperuricemic mice found within the wild or in wild type mice (Lu *et al.*, 2019). This points to the larger problem with the use of animal models in diet-based studies and that is, as a result of evolution and a typical diet lower in fat and protein, mice have multiple differences in the way they absorb, process and excrete various nutrients (National Research Council, 1989). This includes transport proteins and metabolic enzymes that may not only differ from those found in humans but maybe missing entirely in humans as is the case with the uricase enzyme which allows mice to further metabolise uric acid.

The impact this has on our findings is likely to be reduced as due to the nature of cellular models we were able to ensure that the cells were subject to the same level of uric acid exposure, however, this does limit the potential for extrapolation as this difference in nutrient handling provides a degree of uncertainty as to how accurate the replication of the human disease state really is.

4.11 Limitations

Finally, as with all things, it is important to consider potential limitations to this study to ensure that we do not over interpret our data and become too heavily involved in pure speculation. The major limitations that are unique to this study are as follows. Firstly, as all data is based on cell culture of non-primary cell lines this may not provide the full picture as to how these effects may be altered by signalling from other regions within the body such as the pancreas. A second limitation is that we have only used pancreatic cell lines meaning that we cannot guarantee that the exact same trend will be seen in other cell types which will most likely have differing levels of base protein level. A third limitation is purely based on the fact that there is little to no literature that shows exactly how concentrations of intracellular uric acid change when exposed to high extracellular uric acid. We know that it does cause a change in terms of a general increase, however, this has not been well quantified in the literature and was not quantified in this study resulting in potential obscuring of differences between mice and human in regards to the exact change in intracellular uric acid concentrations.

4.12 Additional/ future experimentation

As a final point, we would wish to discuss future experiments that we think would provide greater supporting evidence to our findings which, if we had greater time and budget, would have been performed in addition to the ones in this study. The first of these would be the use of mass

spectrometry analysis to confirm definitively if uric acid was binding to DEPTOR. The second would be to examine how the levels of intracellular uric acid concentration changed as a result of the hyperuricemic condition to allow us to see if this was the same in the mouse and human and if this provided further support for our proposed method, or if this data indicated an alternative possibility we were unable to see based on the data gathered. Thirdly, a more detailed analysis of USP3's effects on DEPTOR through the use of overexpression via a plasmid construct and under expression via silencing RNA. This would allow us to definitively confirm that USP3 is responsible for the changes we see or if it is shown to be insufficient to explain all the changes we observe, and it would provide indications for a more complex signalling pathway. Lastly, we would like to expand the variety of cell types tested in two ways, the simplest being the use of additional cell types from differing regions to analyse if this is purely a local effect isolated to the pancreas or, more likely that this effect may be seen to varying degrees throughout the body. The more complex extension of this would be to use whole animal models and compare the effects of uric acid on DEPTOR expression in tissue samples from multiple regions within mice exposed to chronic hyperuricemia. This step, however, would likely be predicated on the results of initial cell culture-based results which would be used to provide initial expectations in both the potential effect and in how this compares to the effects we would expect to see in humans.

4.13 Conclusion

Finally, as we conclude this report into our findings on the effects of uric acid on DEPTOR ubiquitination we must refer back to our original hypothesis and evaluate if we are able to provide an answer to the central questions from which this study originates. Firstly, does hyperuricemia reduce DEPTOR ubiquitination? Here we can confirm that DEPTOR ubiquitination is reduced by hyperuricemia in both the mouse and human β-cells.

Secondly, that this change of DEPTOR ubiquitination is a result of changes to ubiquitin regulating protein levels. We do have evidence that shows that the expression of USP3 and β-TrCP change significantly under hyperuricemic conditions. The human pancreatic β-cells show a decrease in ubiquitination and increase in deubiquitination which both add to produce a strong DEPTOR stabilising effect that we observed in the reduction of DEPTOR-bound ubiquitin. In the mouse pancreatic β-cell, we see a similar increase in USP3 expression but under human hyperuricemic condition, there was a relative increase in β-TrCP which suggests a blunted response or an alternative mechanism that generated the reduction in DEPTOR-bound ubiquitin. Additionally, we were able to find the first strong evidence that USP3 is a major regulator of DEPTOR deubiquitination.

On the third aspect of our hypothesis, regarding the direct binding of uric acid to DEPTOR, we originally hypothesised that we would not see any direct uric acid binding as at the time there was no existing data to support this idea; and it was less likely that a new type of protein modification would be suggested by this study instead of some indirect interference of uric acid based on its established role as an anti-oxidant. This, however, was demonstrated to be false by both our own work in which we were able to detect protein-bound uric acid in both human and mouse pancreatic β-cells, and by data published by another group over the course of this study.

Lastly, we also put forward the idea that as a result of the changes in DEPTOR ubiquitination we expected to see, we would also expect to see changes in cell viability favouring decreased viability and function to which we saw results that would be largely in line with what we would expect, a decrease in metabolic activity, and β-cell count paired with an increase in apoptosis even if the response in the mouse cells was slightly blunted.

Finally, we would like to present our closing thoughts on this study: we believe that these study results make a strong argument for uric acid being able to modify the ubiquitination of DEPTOR

and that USP3 plays a major role in the regulation of DEPTOR deubiquitination. We hope that this will spark further research into a topic that has been largely ignored and may provide many potential benefits and opportunities for improvement of existing understanding, medical practices, and potential drug targets.

References:

Adnan E, Rahman IA & Faridin HP (2019). Relationship between insulin resistance, metabolic syndrome components and serum uric acid. *Diabetes Metab Syndr Clin Res Rev* **13,** 2158–2162.

de Azevedo MI, Da Silva AS, Ferreiro L, Doleski PH, Tonin AA, Casali EA, Moritz CEJ, Schirmbeck GH, Cardoso V V, Flores MM, Fighera R & Santurio JM (2017). Serum and brain purine levels in an experimental systemic infection of mice by Cryptococcus neoformans: Purinergic immunomodulatory effects. *Microb Pathog* **113,** 124–128.

Bartolome A & Guillén C (2014). *Role of the mammalian target of rapamycin (mTOR) complexes in pancreatic β-cell mass regulation*.

Bernardes SS, de Souza-Neto FP, Ramalho LNZ, Derossi DR, Guarnier FA, da Silva CFN, Melo GP, Simão ANC, Cecchini R & Cecchini AL (2015). Systemic oxidative profile after tumor removal and the tumor microenvironment in melanoma patients. *Cancer Lett* **361,** 226–232.

Berndsen CE & Wolberger C (2014). New insights into ubiquitin E3 ligase mechanism. *Nat Struct Mol Biol* **21,** 301–307.

Bobulescu IA & Moe OW (2012). Renal Transport of Uric Acid: Evolving Concepts and Uncertainties. *Adv Chronic Kidney Dis* **19,** 358–371.

Cameron AJM, Veeriah S, Marshall JJT, Murray ER, Larijani B & Parker PJ (2017). Uncoupling TORC2 from AGC kinases inhibits tumour growth. *Oncotarget* **8,** 84685–84696.

Caron A, Mouchiroud M, Gautier N, Labbé SM, Villot R, Turcotte L, Secco B, Lamoureux G, Shum M, Gélinas Y, Marette A, Richard D, Sabatini DM & Laplante M (2017). Loss of hepatic DEPTOR alters the metabolic transition to fasting. *Mol Metab* **6,** 447–458.

Catena V & Fanciulli M (2017). Deptor: not only a mTOR inhibitor. *J Exp Clin Cancer Res* **36,** 12.

Chevreul K, Berg Brigham K & Bouché C (2014). The burden and treatment of diabetes in France. *Global Health* **10,** 6.

Cicerchi C, Li N, Kratzer J, Garcia G, Roncal-Jimenez CA, Tanabe K, Hunter B, Rivard CJ, Sautin YY, Gaucher EA, Johnson RJ & Lanaspa MA (2014). Uric acid-dependent inhibition of AMP kinase induces hepatic glucose production in diabetes and starvation: Evolutionary implications of the uricase loss in hominids. *FASEB J* **28,** 3339–3350.

Cuadrado A (2015). Structural and functional characterization of Nrf2 degradation by glycogen synthase kinase 3/β-TrCP. *Free Radic Biol Med* **88,** 147–157.

Daviet L & Colland F (2008). Targeting ubiquitin specific proteases for drug discovery. *Biochimie* **90,** 270–283.

Farshi P, Deshmukh RR, Nwankwo JO, Arkwright RT, Cvek B, Liu J & Dou QP (2015). *Deubiquitinases (DUBs) and DUB inhibitors: a patent review*. Available at: http://www.tandfonline.com/doi/full/10.1517/13543776.2015.1056737.

Fathallah-Shaykh SA & Cramer MT (2014). Uric acid and the kidney. *Pediatr Nephrol* **29,** 999–1008.

Frøisland DH, Graue M, Markestad T, Skrivarhaug T, Wentzel-Larsen T & Dahl-Jørgensen K (2013). Health-related quality of life among Norwegian children and adolescents with type 1 diabetes on intensive insulin treatment: a population-based study. *Acta Paediatr* **102,** 889–895.

Fu S, Shao S, Wang L, Liu H, Hou H, Wang Y, Wang H, Huang X & Lv R (2017*a*). USP3 stabilizes p53 protein through its deubiquitinase activity. *Biochem Biophys Res Commun* **492,** 178–183.

Fu S, Shao S, Wang L, Liu H, Hou H, Wang Y, Wang H, Huang X & Lv R (2017*b*). USP3 stabilizes p53 protein through its deubiquitinase activity. ; DOI: 10.1016/j.bbrc.2017.08.036.

He C & Klionsky DJ (2009). Regulation Mechanisms and Signalling Pathways of Autophagy. *Annu Rev Genet* **43,** 67–93.

Heideker J & Wertz IE (2015). DUBs, the regulation of cell identity and disease. *Biochem J* **465,** 1–26.

Huang R & Liu W (2015). Identifying an essential role of nuclear LC3 for autophagy. *Autophagy* **11,** 852–853.

Huber CA, Schwenkglenks M, Rapold R & Reich O (2014). Epidemiology and costs of diabetes mellitus in Switzerland: an analysis of health care claims data, 2006 and 2011. *BMC Endocr Disord* **14,** 44.

Jaberi-Douraki M, Schnell S, Pietropaolo M & Khadra A (2015). Unraveling the contribution of pancreatic beta-cell suicide in autoimmune type 1 diabetes. *J Theor Biol* **375,** 77–87.

Jemth P & Gianni S (2007). PDZ domains: Folding and binding. *Biochemistry* **46,** 8701–8708.

Jia L, Xing J, Ding Y, Shen Y, Shi X, Ren W, Wan M, Guo J, Zheng S, Liu Y, Liang X & Su D (2013). Hyperuricemia Causes Pancreatic B-Cell Death and Dysfunction through NF-kB Signaling Pathway. *PLoS One*; DOI: 10.1371/journal.pone.0078284.

Jiang Y Der, Chang CH, Tai TY, Chen JF & Chuang LM (2012). Incidence and prevalence rates of diabetes mellitus in Taiwan: Analysis of the 2000-2009 Nationwide Health Insurance database. *J Formos Med Assoc* **111,** 599–604.

Johnson RJ, Nakagawa T, Sanchez-Lozada LG, Shafiu M, Sundaram S, Le M, Ishimoto T, Sautin YY & Lanaspa MA (2013). Sugar, uric acid, and the etiology of diabetes and obesity. *Diabetes* **62,** 3307–3315.

Kelly W, Grobner W & Holmes E (1973). Current Conceptd in the Psthogenesis of Hyperuricemia. *Metabolism* **22,** 939–959.

Kodama S, Saito K, Yachi Y, Asumi M, Sugawara A, Totsuka K, Saito A & Sone H (2009). Association between serum uric acid and development of type 2 diabetes. *Diabetes Care* **32,** 1737–1742.

Krishnan E, Akhras KS, Sharma H, Marynchenko M, Wu EQ, Tawk R, Liu J & Shi L (2013). Relative and attributable diabetes risk associated with hyperuricemia in US veterans with gout. *Q J MED* **106,** 721–729.

Krishnan E, Pandya BJ, Chung L, Hariri A & Dabbous O (2012). Hyperuricemia in young adults and risk of insulin resistance, prediabetes, and diabetes: a 15-year follow-up study. *Am J Epidemiol* **176,** 108–116.

Lancini C, van den Berk PCM, Vissers JHA, Gargiulo G, Song J-Y, Hulsman D, Serresi M, Tanger E, Blom M, Vens C, van Lohuizen M, Jacobs H & Citterio E (2014). Tight regulation of ubiquitin-mediated DNA damage response by USP3 preserves the functional integrity of hematopoietic stem cells. *J Exp Med* **211,** 1759–1777.

Leney AC, El Atmioui D, Wu W, Ovaa H & Heck AJR (2017). Elucidating crosstalk mechanisms between phosphorylation and O-GlcNAcylation. *Proc Natl Acad Sci* **114,** E7255–E7261.

Li H, Sun GY, Zhao Y, Thomas D, Greenson JK, Zalupski MM, Ben-Josef E & Sun Y (2014). DEPTOR has growth suppression activity against pancreatic cancer cells. *Oncotarget* **5,** 12811–12819.

Li Z, Shen Y, Chen Y, Zhang G, Cheng J & Wang W (2018). High Uric Acid Inhibits Cardiomyocyte Viability Through the ERK/P38 Pathway via Oxidative Stress. *Cell Physiol Biochem*1156–1164.

Liu J, Shaik S, Dai X, Wu Q, Zhou X, Wang Z & Wei W (2015). Targeting the Ubiquitin Pathway for Cancer Treatment. *Biochim Biophys Acta* **1855,** 50–60.

Lõpez De Figueroa P, Lotz MK, Blanco FJ & Caramés B (2015). Autophagy activation and protection from mitochondrial dysfunction in human chondrocytes. *Arthritis Rheumatol* **67,** 966–976.

Low W, Lee Y & Samy AL (2015). Non-communicable diseases in the Asia-Pacific region: Prevalence, risk factors and community-based prevention. *Int J Occup Med Environ Health* **28,** 20–26.

Lu J, Dalbeth N, Yin H, Li C, Merriman TR & Wei WH (2019). Mouse models for human hyperuricaemia: a critical review. *Nat Rev Rheumatol* **15,** 413–426.

Maiuolo J, Oppedisano F, Gratteri S, Muscoli C & Mollace V (2016). Regulation of uric acid metabolism and excretion. *Int J Cardiol* **213,** 8–14.

Masini M, Bugliani M, Lupi R, Del Guerra S, Boggi U, Filipponi F, Marselli L, Masiello P & Marchetti P (2009). Autophagy in human type 2 diabetes pancreatic beta cells. *Diabetologia* **52,** 1083–1086.

McCluskey JT, Hamid M, Guo-Parke H, McClenaghan NH, Gomis R & Flatt PR (2011). Development and functional characterization of insulin-releasing human pancreatic beta cell lines produced by electrofusion. *J Biol Chem* **286,** 21982–21992.

Melikian M, Eluard B, Bertho G, Baud V & Evrard-Todeschi N (2017). Model of the Interaction between the NF-κB Inhibitory Protein p100 and the E3 Ubiquitin Ligase β-TrCP based on NMR and Docking Experiments. *J Chem Inf Model* **57,** 223–233.

Motojima K & Goto S (1990). Characterization of liver-specific expression of rat uricase using monoclonal antibodies and cloned cDNAs. *BBA - Gene Struct Expr* **1087,** 316–322.

Munnee K, Bundhun PK, Quan H & Tang Z (2016). Comparing the clinical outcomes between insulin-treated and non-insulin-treated patients with type 2 diabetes mellitus after coronary artery bypass surgery: A systematic review and meta-analysis. *Med (United States)*; DOI: 10.1097/MD.0000000000003006.

Munson MJ & Ganley IG (2015). MTOR, PIK3C3, and autophagy: Signaling the beginning from the end. *Autophagy* **11,** 2375–2376.

Musacchio E, Perissinotto E, Sartori L, Veronese N, Punzi L, Zambon S, MANZATO E, Baggio G, Corti M-C, Crepaldi G & Ramonda R (2016). Hyperuricemia, cardiovascular profile, and comorbidity in older men and women: the Pro.V.A. Study. *Rejuvenation Res* **20,** 42–49.

National Research Council (1989). Nutrient Requirements of the Horse. *J Equine Vet Sci* **9,** 288.

Neutzner M & Neutzner A (2012). Enzymes of ubiquitination and deubiquitination. *Essays Biochem* **52,** 37–50.

Ohtake F, Saeki Y, Sakamoto K, Ohtake K, Nishikawa H, Tsuchiya H, Ohta T, Tanaka K & Kanno J (2015). Ubiquitin acetylation inhibits polyubiquitin chain elongation. *EMBO Rep* **16,** 192–201.

Ohtsubo K & Marth JD (2006). Glycosylation in Cellular Mechanisms of Health and Disease. *Cell* **126,** 855–867.

Olmos P, A'Hern R, Heaton D., Millward B., Risley D, Leslie RD & Pyke DA (1988). The significance of the concordance rate for Type 1 (insulin-dependent) diabetes in identical twins. *Diabetologia* **1,** 747–750.

Papanas N & Ziegler D (2015). Risk factors and comorbidities in diabetic neuropathy: An update 2015. *Rev Diabet Stud* **12,** 48–62.

Peterson T, Laplante M, Thoreen C, Sancak Y, Kang S, Kuehl M, Grey N & Sabatini D (2009). DEPTOR is an mTOR Inhibitor Whose Frequent Overexpression in Multiple Myeloma Cells Promotes their Survival. *Cell* **137,** 873–886.

Pipeleers D, Chintinne M, Denys B, Martens G, Keymeulen B & Gorus F (2008). Restoring a functional β-cell mass in diabetes. *Diabetes, Obes Metab* **10,** 54–62.

Qiu M, Shen W, Song X, Ju L, Tong W, Wang H, Zheng S, Jin Y, Wu Y, Wang W & Tian J (2015). Effects of Prediabetes Mellitus Alone or Plus Hypertension on Subsequent Occurrence of Cardiovascular Disease and Diabetes Mellitus Longitudinal Study. *Hypertension* **65,** 622–628.

Ravanan P, Srikumar IF & Talwar P (2017). Autophagy: The spotlight for cellular stress responses. *Life Sci* **188,** 53–67. Available at: http://dx.doi.org/10.1016/j.lfs.2017.08.029 [Accessed November 27, 2018].

Rojas J, Bermudez V, Palmar J, Martínez MS, Olivar LC, Nava M, Tomey D, Rojas M, Salazar J, Garicano C & Velasco M (2018). Pancreatic beta cell death: Novel potential mechanisms in diabetes therapy. *J Diabetes Res* **2018,** 19. Available at: https://doi.org/10.1155/2018/9601801 [Accessed June 25, 2019].

Rojnic Putarek N, Ille J, Spehar Uroic A, Skrabic V, Stipancic G, Krnic N, Radica A, Marjanac I, Severinski S, Svigir A, Bogdanic A & Dumic M (2015). Incidence of type 1 diabetes mellitus in 0 to 14-yr-old children in Croatia - 2004 to 2012 study. *Pediatr Diabetes* **16,** 448–453.

Saisho Y, Butler AE, Manesso E, Elashoff D, Rizza RA & Butler PC (2013). β-Cell mass and turnover in humans: Effects of obesity and aging. *Diabetes Care* **36,** 111–117.

Sato Y, Goto Y, Narita N & Hoon DSB (2009). Cancer cells expressing toll-like receptors and the tumor microenvironment. In *Cancer Microenvironment*. Available at: https://link-springer-com.ezproxy.otago.ac.nz/content/pdf/10.1007%2Fs12307-009-0022-y.pdf [Accessed June 21, 2019].

Schipf S, Ittermann T, Tamayo T, Holle R, Schunk M, Maier W, Meisinger C, Thorand B, Kluttig A, Greiser KH, Berger K, Müller G, Moebus S, Slomiany U, Icks A, Rathmann W & Völzke H (2014). Regional differences in the incidence of self-reported type 2 diabetes in Germany: results from five population-based studies in Germany (DIAB-CORE Consortium). *J Epidemiol Community Health* **68,** 1088–1095.

Sevanian A, Davies KJA & Hochstein P (1985). Conservation of vitamin C by uric acid in blood. *J Free Radicals Biol Med* **1,** 117–124.

Sheng YL, Chen X, Hou XO, Yuan X, Yuan BS, Yuan YQ, Zhang QL, Cao X, Liu CF, Luo WF & Hu LF (2017). Urate promotes SNCA/α-synuclein clearance via regulating mTOR-dependent macroautophagy. *Exp Neurol* **297,** 138–147.

Shimodaira M, Niwa T, Nakajima K, Kobayashi M, Hanyu N & Nakayama .T (2014). The Relationship Between Serum Uric Acid Levels and β-Cell Functions in Nondiabetic Subjects. *Horm Metab Res*950–954.

Sloper-mould KE, Eyre HJ, Wang XW, Sutherland GR & Baker RT (1999). Characterization and chromosomal localization of USP3, a novel human ubiquitin-specific protease. *J Biol Chem* **274,** 26878–26884.

So A & Thorens B (2010). Science in medicine Uric acid transport and disease. *J Clin Invest* **120,** 1791–1799.

Soltani Z, Rasheed K, Kapusta DR & Reisin E (2013). Potential role of uric acid in metabolic syndrome, hypertension, kidney injury, and cardiovascular diseases: Is it time for reappraisal? *Curr Hypertens Rep* **15,** 175–181.

Spiga R, Marini MA, Mancuso E, Di Fatta C, Fuoco A, Perticone F, Andreozzi F, Mannino GC & Sesti G (2017). Uric Acid Is Associated with Inflammatory Biomarkers and Induces Inflammation Via Activating the NF-κB Signaling Pathway in HepG2 Cells. *Arterioscler Thromb Vasc Biol* **37,** 1241–1249.

Tae WY, Ki CS, Hun SS, Byung JK, Bum SK, Jin HK, Man HL, Jung RP, Kim H, Eun JR, Won YL, Sun WK, Seung HR & Dong GK (2005). Relationship between serum uric acid concentration and insulin resistance and metabolic syndrome. *Circ J* **69,** 928–933.

Takahiro Shintani & Klionsky DJ (2004). Autophagy in Health and Disease: A Double-Edged Sword Takahiro. *Science (80-)* **306,** 990–995.

Thomas MC, Brownlee M, Susztak K, Sharma K, Jandeleit-Dahm KAM, Zoungas S, Rossing P, Groop P-H & Cooper ME (2015). Diabetic kidney disease. *Nat Rev Dis Prim* **1,** 1–20.

Turner R, Brennan SO, Ashby L V, Dickerhof N, Hamzah MR, Pearson JF, Stamp LK & Kettle AJ (2018). Conjugation of urate-derived electrophiles to proteins during normal metabolism and inflammation. *J Biol Chem* **293,** 19886–19898.

Varadaiah YGC, Sivanesan S, Nayak SB & Thirumalarao KR (2019). Purine metabolites can indicate diabetes progression. *Arch Physiol Biochem*1–5.

Varusai TM & Nguyen LK (2018). Dynamic modelling of the mTOR signalling network reveals complex emergent behaviours conferred by DEPTOR. *Sci Rep* **8,** 1–14.

Vergès B & Cariou B (2015). MTOR inhibitors and diabetes. *Diabetes Res Clin Pract* **110,** 101–108.

Vijayakumar TM, Jayram J, Meghana Cheekireddy V, Himaja D, Dharma Teja Y & Narayanasamy D (2017). Safety, Efficacy, and Bioavailability of Fixed-Dose Combinations in Type 2 Diabetes Mellitus: A Systematic Updated Review. *Curr Ther Res* **84,** 4–9.

Wang X, Misawa R, Zielinski MC, Cowen P, Jo J, Periwal V, Ricordi C, Khan A, Szust J, Shen J, Millis JM, Witkowski P & Hara M (2013). Regional Differences in Islet Distribution in the Human Pancreas - Preferential Beta-Cell Loss in the Head Region in Patients with Type 2 Diabetes. *PLoS One* **8,** 1–9.

Wang Z, Zhong J, Gao D, Inuzuka H, Liu P & Wei W (2012). DEPTOR ubiquitination and destruction by SCF -TrCP. *AJP Endocrinol Metab* **303,** E163–E169.

Wright AF, Rudan I, Hastie ND & Campbell H (2010). A 'complexity' of urate transporters. *Kidney Int* **78,** 446–452.

Wu Y, Ding Y, Tanaka Y & Zhang W (2014). Risk factors contributing to type 2 diabetes and recent advances in the treatment and prevention. *Int J Med Sci* **11,** 1185–1200.

Yang X, Wood PA, Ansell CM, Ohmori M, Oh E-Y, Xiong Y, Berger FG, Pena MMO & Hrushesky WJM (2009). -Catenin Induces -TrCP-Mediated PER2 Degradation Altering Circadian Clock Gene Expression in Intestinal Mucosa of ApcMin/+ Mice. *J Biochem* **145,** 289–297.

Yao H, Tang H, Zhang Y, Zhang QF, Liu XY, Liu YT, Gu WT, Zheng YZ, Shang HB, Wang Y, Huang JY, Wei YX, Zhang X, Zhang J & Wu ZB (2019). DEPTOR inhibits cell proliferation and confers sensitivity to dopamine agonist in pituitary adenoma. *Cancer Lett* **459,** 135–144.

Zhai Y, Lin P, Feng Z, Lu H, Han Q, Chen J, Zhang Y, He Q, Nan G, Luo X, Wang B, Feng F, Liu F, Chen Z & Zhu P (2018). TNFAIP3-DEPTOR complex regulates inflammasome secretion through autophagy in ankylosing spondylitis monocytes. *Autophagy* **14,** 1629–1643.

Zhang Q et al. (2016). The predictive value of mean serum uric acid levels for developing prediabetes. *Diabetes Res Clin Pract* **118,** 79–89.

Zhang W & Sidhu SS (2014). Development of inhibitors in the ubiquitination cascade. *FEBS Lett* **588,** 356–367.

Zhao L, Wang X, Yu Y, Deng L, Chen L, Peng X, Jiao C, Gao G, Tan X, Pan W, Ge X & Wang P (2018). OTUB1 protein suppresses mTOR complex 1 (mTORC1) activity by deubiquitinating the mTORC1 inhibitor DEPTOR. *J Biol Chem* **293,** 4883–4892.

Zhao Y & Sun Y (2012). Targeting the mTOR-DEPTOR pathway by CRL E3 ubiquitin ligases: therapeutic application. *Neoplasia* **14,** 360–367.

Zhao Y, Xiong X & Sun Y (2005). DEPTOR, an mTOR inhibitor, is a physiological substrate of SCFβTrCP E3 ubiquitin ligase and regulates survival and autophagy. *Biophys Chem* **257,** 2432–2437.

Zhu Y, Pandya BJ & Choi HK (2011). Prevalence of gout and hyperuricemia in the US general population: The National Health and Nutrition Examination Survey 2007-2008. *Arthritis Rheum* **63,** 3136–3141.

Zoncu R, Efeyan A & Sabatini DM (2011). MTOR: From growth signal integration to cancer, diabetes and ageing. *Nat Rev Mol Cell Biol* **12,** 21–35. Available at: www.nature.com/reviews/molcellbio [Accessed June 21, 2019].

Appendices

Appendix 1. **Expanded western blots.**

Expanded protein band and ladder. In the case of some blots, the ladder is shared.

1.1B4
UB
(Figure 7,Page 38)

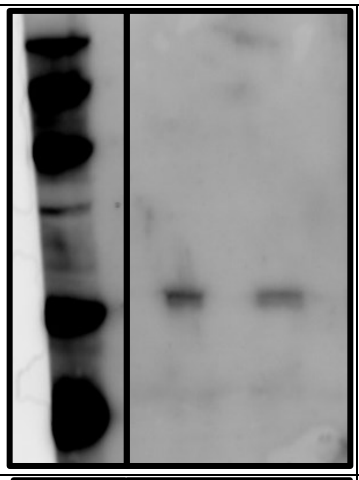

MIN6
UB
(Figure 7, Page 38)

1.1B4
UA
(Figure 9, Page 42)

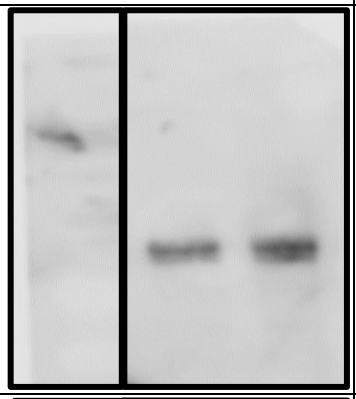

MIN6
UA
(Figure 9, Page 42)

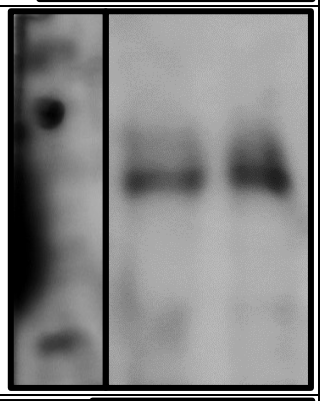

1.1B4
UA/UB DEPTOR
(Figure 7, Page 38)
(Figure 9, Page 42)

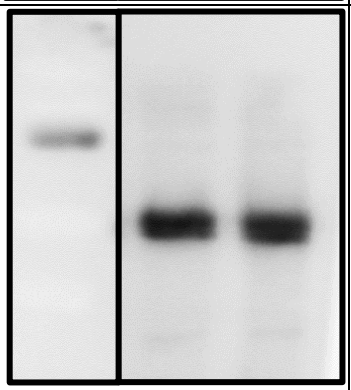

MIN6
UA/UB DEPTOR
(Figure7, Page 38)
(Figure 9, Page 42)

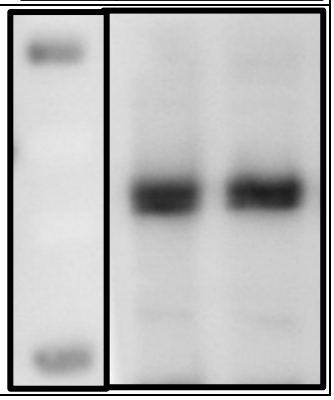

1.1B4 **USP3** (Figure 8, Page 40)	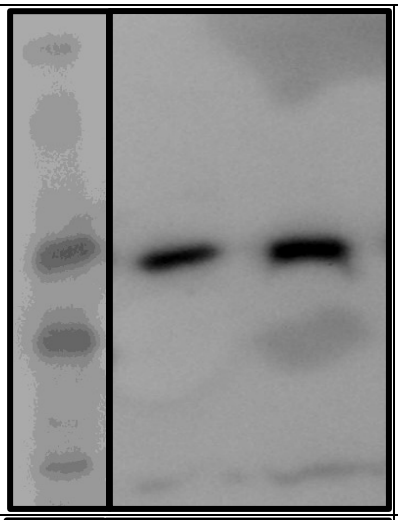
MIN6 **USP3** (Figure 8, Page 40)	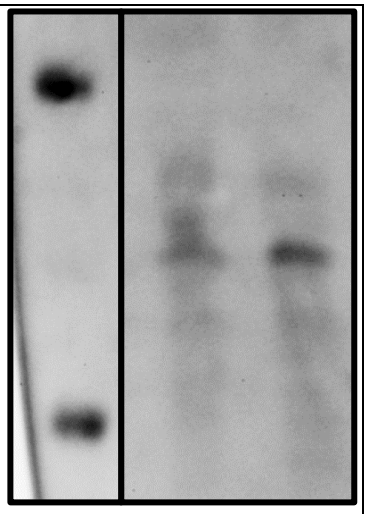
1.1B4 **USP3 GAPDH** (Figure 8, Page 40)	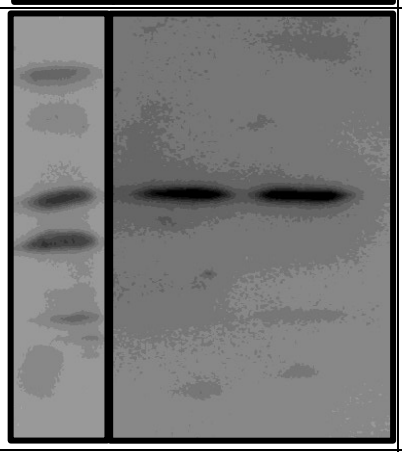
MIN6 **USP3 GAPDH** (Figure 8, Page 40)	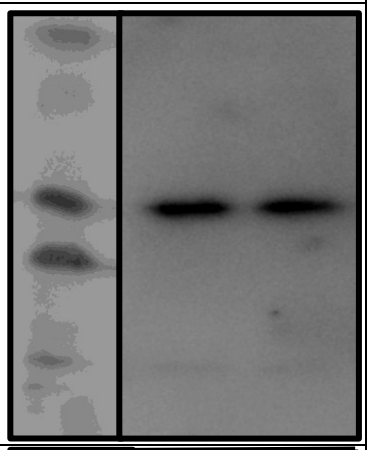
1.1B4 **β-TrCP** (Figure 8, Page 40)	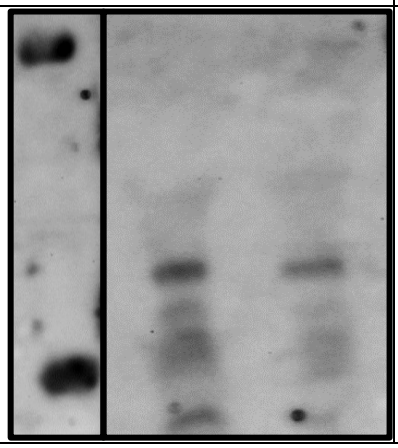
MIN6 **β-TrCP** (Figure 8, Page 40)	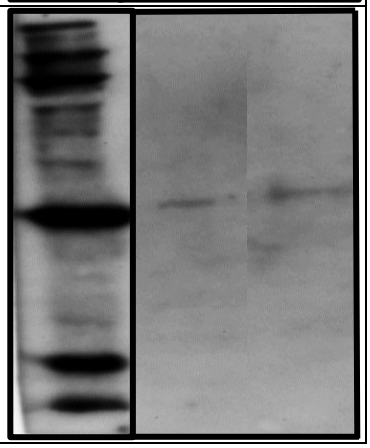

1.1B4
β-TrCP GAPDH
(Figure 8, Page 40)

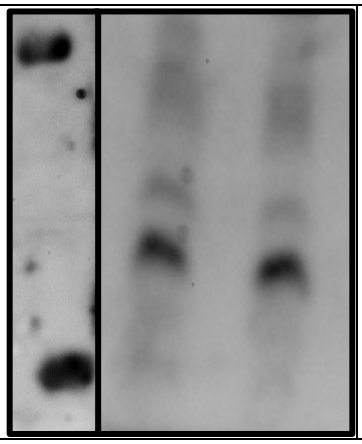

MIN6
β-TrCP GAPDH
(Figure 8, Page 40)